I

SAND77-1423

SUSTAINED MOLTEN STEEL/CONCRETE INTERACTIONS TESTS

A Preliminary Report on the Feasibility of Experimental Techniques

DANA A. POWERS

Prepared by Sandia Laboratories, Albuquerque, New Mexico 87115
and Livermore, California 94550 for the United States Energy Research
and Development Administration under Contract AT (29-1)-789

June 1978

Sandia Laboratories

SF 2900 Q(7-73)

Prepared for

U. S. NUCLEAR REGULATORY COMMISSION

NOTICE

The views expressed in this report are not necessarily those of the U.S. Nuclear Regulatory Commission.

Available from
National Technical Information Service
Springfield, Virginia 22161

NUREG/CR-0166
SAND77-1423
R-3

SUSTAINED MOLTEN STEEL/CONCRETE INTERACTIONS TESTS

A Preliminary Report on the Feasibility of Experimental Techniques

Dana A. Powers

Date Published: June 1978

Sandia Laboratories
Albuquerque, New Mexico 87185
operated by
Sandia Corporation
for the
U. S. Department of Energy

Prepared for
Division of Reactor Safety Research
Office of Nuclear Regulatory Research
U.S. Nuclear Regulatory Commission
Washington, D.C. 20555
Under Interagency Agreement DOE 40-550-75
NRC FIN No. A1019

ABSTRACT

An experimental demonstration of the feasibility of using induction heating to maintain 200 kilograms of stainless steel molten while in contact with concrete is described. Data are presented to show that operation of an induction coil embedded in the concrete at 120 kW was sufficient to sustain temperatures near 1500°C in the melt for 10 minutes. Metal losses by gas induced expulsion from the crucible and oxidation may have been responsible for the inability to achieve higher temperatures.

Techniques for monitoring melt temperatures, the compositions and temperatures of evolved gases, and concrete temperatures during the test are described. Gases generated during the test were chemically reduced and contained substantial amounts of methane and ethene in addition to the expected species hydrogen, carbon monoxide and carbon dioxide. Observations made during and after the test suggest that these evolved gases may have played an important role in determining the nature of melt attack on the concrete.

Concrete used in the test, a calcareous variety representative of that found in the southeastern United States, is characterized in terms of its composition and thermochemical behavior. Melting in this concrete is shown to begin at 1340 ± 10°C. Liquidus is reached at temperatures near 1600 ± 30°C.

CONTENTS

I. INTRODUCTION

Exploratory tests in which large steel melts were teemed into concrete crucibles have revealed a variety of phenomena pertinent to questions of the safety of light-water and fast nuclear reactors (1-8). To quantitatively evaluate these phenomena and to explore the time evolution of the phenomena, it is desirable to maintain the steel molten while in contact with concrete for periods longer than allowed by natural cooling in the previous, transient tests. One method for sustaining melt/concrete interactions is to inductively heat the melt once it is in contact with the concrete.

A test utilizing this inductive heating method to maintain 200 kilograms of Type 304 stainless steel in the molten state while in contact with calcareous concrete representative of that found in the Southeastern United States has been conducted. This test, designated COIL-1 and the first in a series of four, has also demonstrated the utility of experimental techniques to monitor melt temperatures, chemical compositions and temperatures of evolved gases, and concrete temperatures.

In response to interest among members of the reactor safety community in the outcome of the feasibility test, this preliminary report of the test results is presented. Observations, data and interpretations found herein have been subjected to neither careful scrutiny nor the tests of replicative and confirmatory experimentation. Great caution along with a clear recognition of the limits of the test should be invoked before these results are extrapolated to other situations.

II DESCRIPTION OF THE EXPERIMENTAL APPARATUS AND PROCEDURE

The concrete crucible was the heart of the experimental apparatus used in this test designated COIL-1. The design of the crucible is schematically shown in Figure 1. The crucible was a cylindrical block of concrete 73.7 cm high and 83.8 cm in diameter with a coaxial, cylindrical cavity 38.1 cm deep and 38.1 cm in diameter. A coaxial induction coil was embedded in the concrete 11.4 cm below the top of the crucible. The coil was designed and built by Inductotherm, Inc. (see Figure 2a). It consisted of 11 turns of epoxy-coated copper tubing 3.2 cm in diameter Turns of the coil were maintained in separation by three Transite spacers located symmetrically about the coil. The coil was 43.2 cm high and had an inside diameter of 58.4 cm. The coil was swathed in asbestos paper 0.16 cm thick to prevent puncture of the epoxy resin on the copper tubes during crucible fabrication (see Figure 2b).

Walls of the crucible cavity were separated from the coil by 10.2 cm of concrete. Total wall thickness of the crucible was 17.8 cm. The base was 35.5 cm thick. The coil extended 16.5 cm below the bottom of the crucible cavity so that as melt penetrated downward during the test it was retained in the inductive field of the coil. The crucible was not equipped with reinforcement save that provided by the coil.

The crucible design represents a compromise between the conflicting requirements that there be good electrical coupling between the melt and the induction coil, and that the crucible walls be sufficiently thick that fracture would not occur during the test. Because the

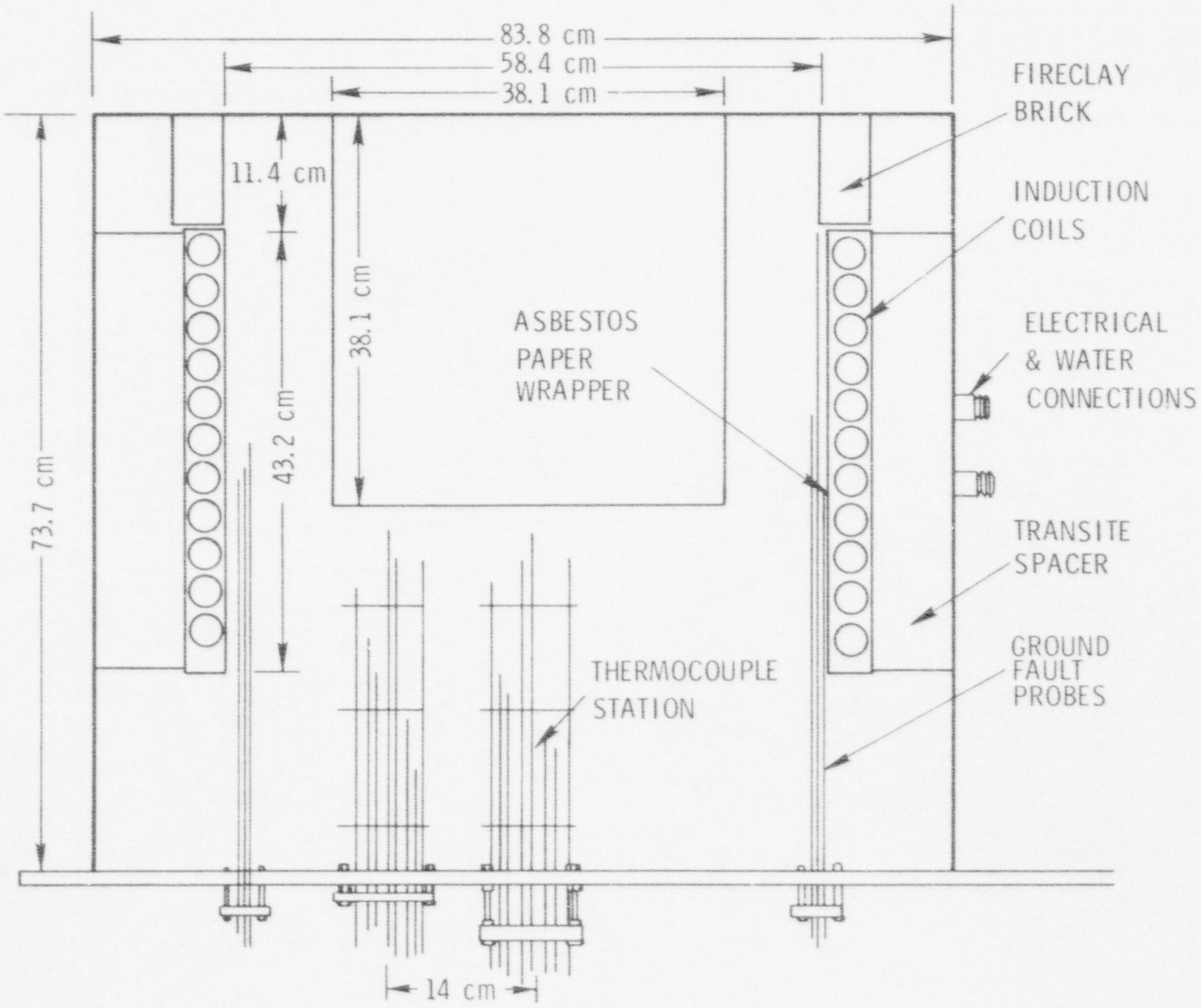

FIGURE 1 - CROSS SECTIONAL SIDE VIEW OF FIXTURE FOR THE SUSTAINED MOLTEN STEEL CONCRETE INTERACTION

FIGURE 2 - INDUCTION COIL USED IN TEST COIL-1.

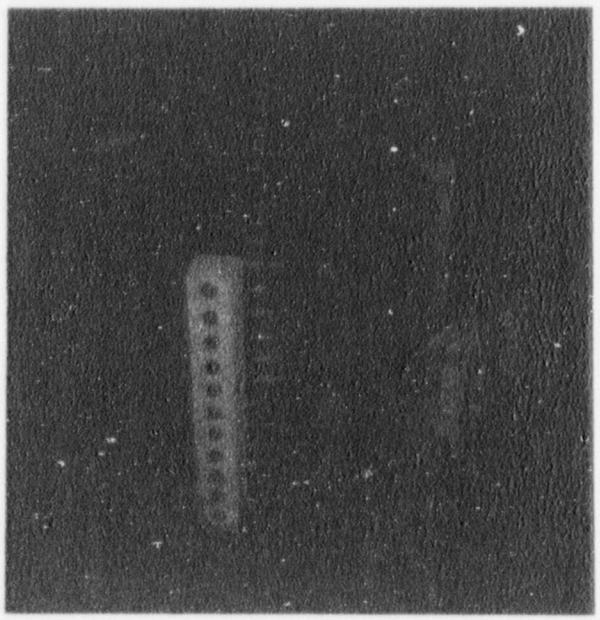

a) Bare induction coil showing Transite spacers and the power and water connections.

b) Coil swathed in asbestos paper.

induction coil is water-cooled to a temperature of less than 60°C, its presence could distort heat transfer from a melt in the crucible in such a way that radial expansion of the melt is artifically depressed. The thickness of concrete initially separating melt from the coil in this test was designed to be 2-1/2 to 3 times the maximum thickness of the zone of thermally altered concrete observed in transient melt/concrete interactions tests (1-7). Sustained tests using this crucible design should be free of any significant heat-transfer distortion due to the presence of the coil for testing times of at least 18 to 27 minutes.

Melt migration into the vicinity of the coils was a major safety concern. Should a water-cooled coil turn rupture, a vigorous melt-water interaction might occur. To avoid this, six ground-fault probes were located adjacent to the inner surface of the induction coil. Shut-down of the experiment was dictated should current in these 3 mm diameter type 304 stainless steel detectors exceed 90 milliamperes. Shut-down was also dictated if the coil cooling water temperature exceeded 60°C.

Concrete used in the manufacture of the crucible was a calcareous variety generic to the southeastern United States. Its bulk composition and aggregate specifications are listed in Tables 1-3. These specifications conform to those described by the Breeder Reactor Division of Burns and Roe, Inc., for concrete in the Clinch River Breeder Reactor (9). Concrete for the crucible was prepared at the Civil Engineering Research Facility operated by the University of New Mexico. Strengths of the concrete after 28 and 90 days of cure exceeded 27.5 and 41.2 MPa,

TABLE 1

BULK COMPOSITION OF CONCRETE

Type II Portland Cement		279 kg/m^3
Fly Ash		47.6 kg/m^3
Fine Aggregate	Tennessee Limestone	773 kg/m^3
Coarse Aggregate	Tennessee Limestone	1083 kg/m^3
Water Reducing Agent (Plastimet - Sika Chemical Co.)		545 cm^3/m^3
Air Entraining Agent (Resex - Hunt Process Co.)		541 cm^3/m^3
Total Water		158 - 174 kg/m^3

TABLE 2

COARSE AGGREGATE SPECIFICATIONS

Tennessee Limestone

Sieve Designation (Square Opening)	Percent by Weight Passing Sieve
2.5 cm	100
1.9 cm	90 - 100
0.95 cm	20 - 55
0.48 cm	0 - 10
0.23 cm	0 - 5

TABLE 3

FINE AGGREGATE SPECIFICATIONS

Ground Tennessee Limestone

Sieve Designation (Square Opening)	Percent by Weight Passing Sieve
0.95 cm	100
0.48 cm	95 - 100
0.23 cm	80 - 100
0.12 cm	50 - 85
0.058 cm	25 - 60
0.030 cm	10 - 30
0.015 cm	2 - 10

respectively. Density of the concrete determined from 15.2 cm diameter, 30.4 cm high testing cylinders was 2.40 ± 0.03 g/cm^3. The concrete had cured 219 days at the time of the test.

As temperature is increased this concrete undergoes decomposition to yield volatile products in three distinct steps. The thermogram in Figure 3 shows a weight loss of about 3% in the temperature range of 30-230°C which may be assigned to loss of evaporable water. A weight loss of about 1% centered at 420°C may be assigned to the loss of water from calcium hydroxide in the cementituous phases of the concrete. The final weight loss, which amounts to 36.5% of the sample, is due to decarboxylation of cement and aggregate in the concrete. The molar ratio of water to carbon dioxide in the concrete is about 0.27.

A differential thermogram of the concrete is shown in Figure 4. Endotherms at ~ 100, 470 and 650°C are due to the three decomposition reactions described above. A small endothermic peak at 800°C may be due to decomposition of dolomite ($MgCa(CO_3)_2$)[10] known to contaminate the calcareous aggregate. No endotherm due to the $\alpha \rightarrow \beta$ phase change of free silicon dioxide could be detected at the sensitivity used in acquiring this thermogram. Weak endotherms which peak at 1240 and 1320°C may be due to reactions among the very heterogeneous solid decomposition products of concrete. The final, intense endotherm is due to melting of these decomposition products. The onset of melting occurs at 1340 ± 10°C. Liquidus temperature of the mixture is difficult to determine accurately but appears to occur at 1600 ± 30°C.

Comparison of the relative areas enclosed by melting endotherms of the concrete and calcium fluoride (melting point = 1382°C; enthalpy of fusion = 52.5 cal/gm) provides an estimate of the enthalpy of fusion

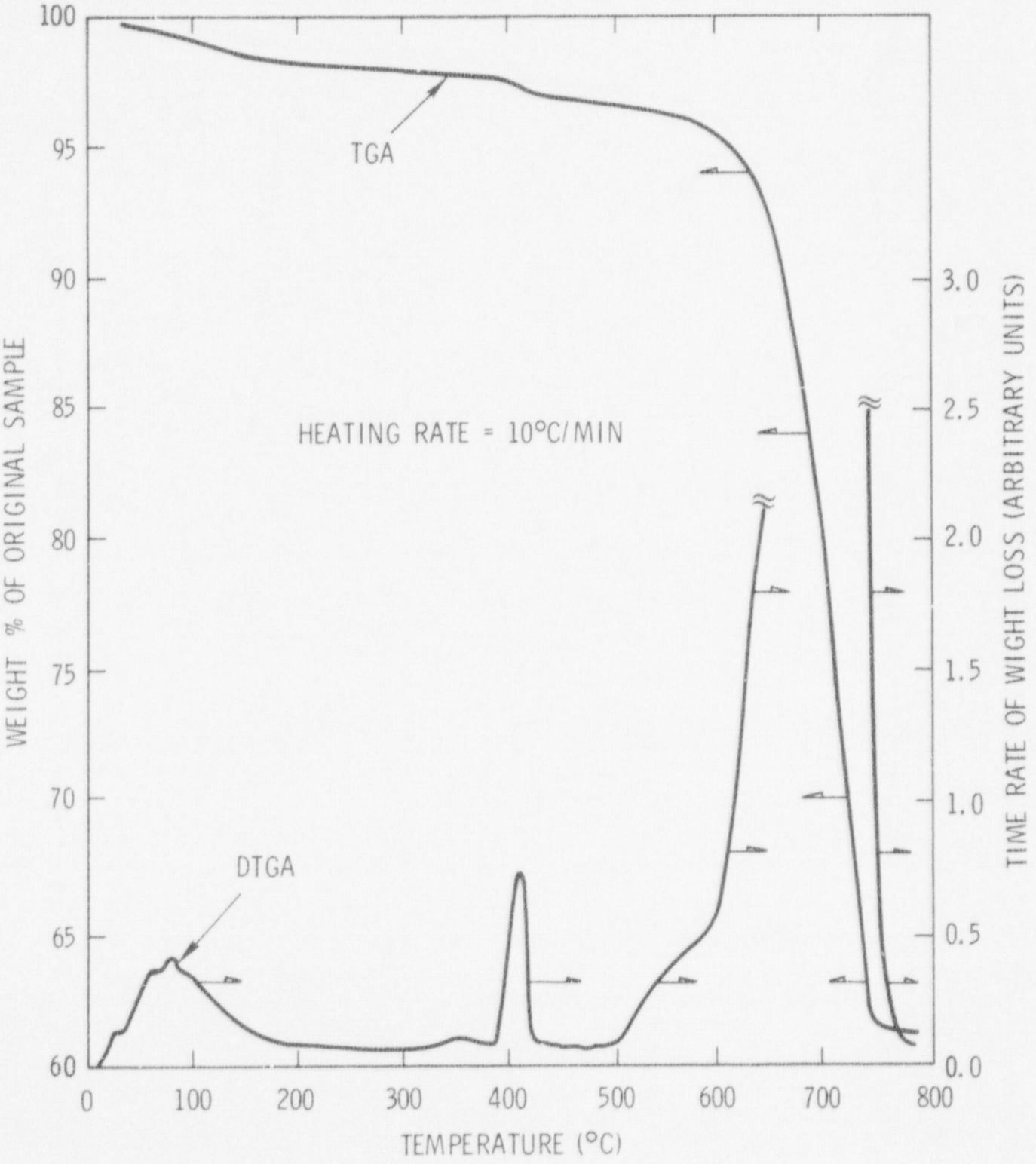

FIGURE 3. THERMOGRAM OF CONCRETE USED IN TEST COIL-1.

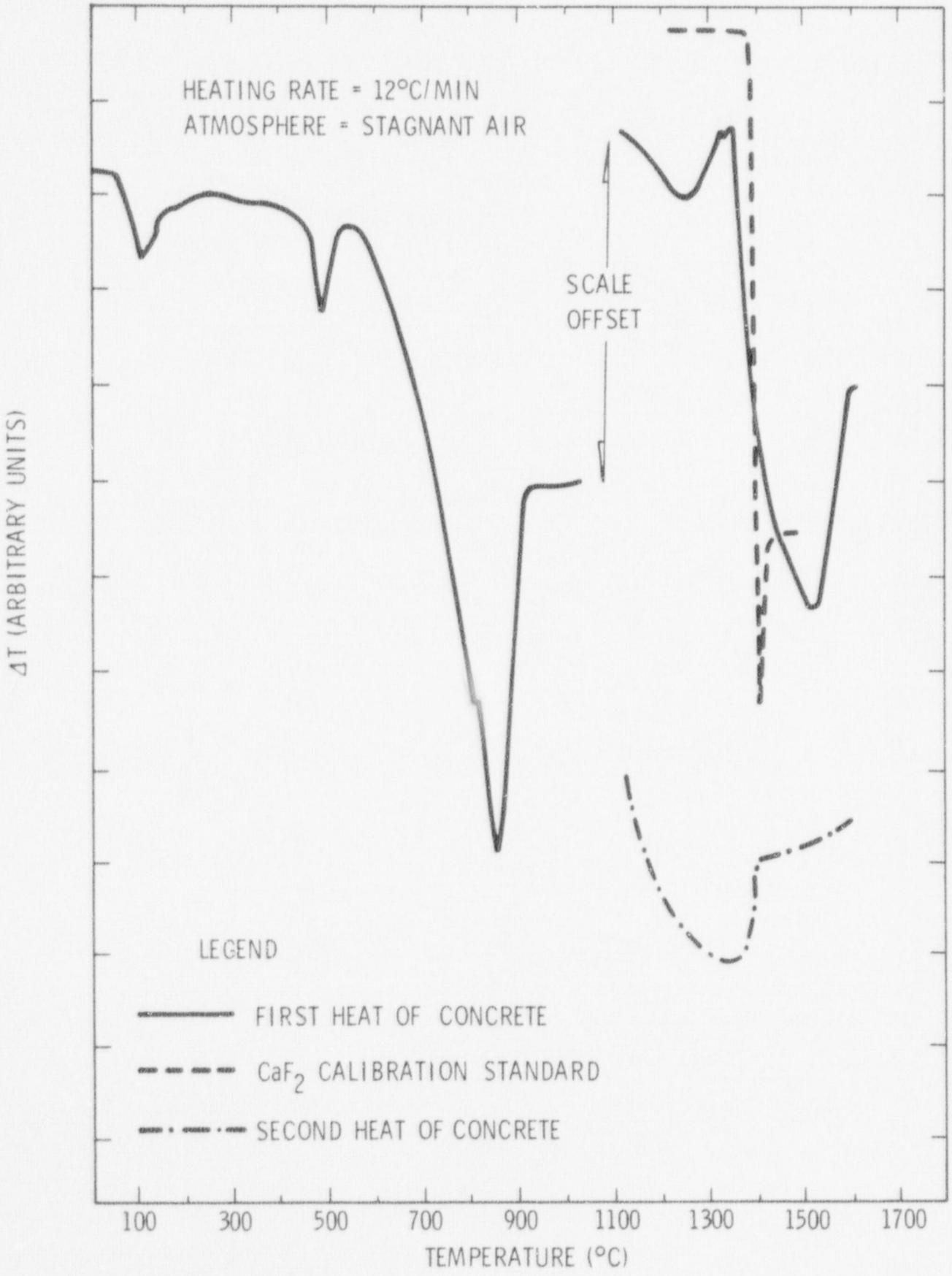

FIGURE 4. DIFFERENTIAL THERMOGRAM OF CONCRETE USED IN TEST COIL-1.

of concrete of 250 ± 75 cal per gram of virgin concrete or 410 ± 125 cal per gram of solid concrete decomposition products. This is almost certainly a high estimate.

The product of fusing concrete is a heterogeneous material which, upon solidification and reheating, undergoes a second order phase change at 1370°C (see Figure 4).

The melt used in test COIL-1 was made from a 205 kg type 304 stainless steel ingot. The melt was formed in a 165 kW, 1000 Hz induction furnace custom manufactured by Cheston, Inc. The furnace crucible was made of a magnesium oxide-based ceramic. Temperatures were monitored during melt preparation with silica sheathed, disposable, Type S immersion thermocouples (Leeds and Northrup "Dip-Tips"). When melt temperature reached 1720 ± 5°C, hydraulic equipment was used to teem the crucible contents into the awaiting test crucible. The moment melt came into contact with the concrete was used to mark the start of the test. Furnace contents were completely expelled 17.1 seconds after the start of the test. Once the teem was complete the power supply used with the furnace was switched to energize the induction coil in the concrete crucible. Design limits of the power supply restricted operation of the embedded coil to power levels of less than 125 kW. Throughout the sustained portion of test COIL-1 the coil was operated at 120 kW. No indication of the efficiency of electrical coupling between the coil and the melt was available in this test. Monitors of cooling water temperature, coil power, voltage and frequency indicated that no serious difficulties were encountered in this coupling.

The sustained portion of the test was terminated 10 minutes after the start when current in the ground fault detection probes exceeded 90 milliamperes.

Since COIL-1 was a feasibility test, instrumentation to monitor the melt/concrete interaction was limited to the following devices:

1. Immersion, in situ, and pyrometric monitors of the melt temperature.
2. Monitors of the gas phase temperatures.
3. Sampling devices for determination of the gas phase composition.
4. Concrete temperature monitors.
5. Photographic and videotape recording of the test events.

High-frequency noise emitted by the induction coil in the crucible greatly complicated use of readily available instrumentation in a sustained test. Stray output from the coil can introduce noise into electrical signals from the instruments. This is especially bothersome with thermocouples. The stray output also can couple with conductive, and especially magnetic, materials causing them to be heated even when several feet from the coil. Careful grounding and material selection practices were necessary to avoid these difficulties. Metallic materials were chosen to be stainless steel or, where possible, aluminum. Where feasible, grooves were cut in the metal to break up electric currents induced by the coil field.

Immersion melt-temperature thermocouples were identical to those used to monitor temperatures during furnace preparation of the melt. These devices had been successfully used to make up to nine temperature measurements in transient melt/concrete interactions tests. In the

sustained test, however, both the operator and device electrics were subjected to much more intense heating which limited the efficacy of the immersion device to three measurements.

A schematic diagram of the in situ melt thermocouple is shown in Figure 5. The sensing element was a type S thermocouple insulated with MgO and sheathed in a 0.16 cm OD Pt-6% Rh alloy tube. The tube was embedded in a mixture of 50 w/o silicon carbide - 50 w/o aluminum oxide powder contained in a 1.26 cm OD, 0.63 ID mullite protection tube. The protection tube was also embedded in SiC-Al_2O_3 powder within a 4.4 cm OD, 2.54 cm ID sacrificial silicon carbide tube. The mullite protection tube was intended to separate the sensor from the chemical environment presented by the test. The silicon carbide tube shielded the protection tube from thermal shock during the melt deposition into the crucible. The sensor assembly was located in the crucible cavity within a fireclay block.

Post-test inspection of the in situ fixture showed that it had survived the chemical and thermal shock environment of the test but had been failed by some mechanical stress on the joint connecting the fixture to the crucible.

A Pyrometer Instrument Co. model Photo II pyrometer was focused on the melt surface at an angle of 36° to the top of the crucible and 6.1 meters from the crucible cavity. Data collected by this device were difficult to interpret since emissions at the 650 nm operating wavelength from both the melt and flames formed in the test could be responsible for output from the device.

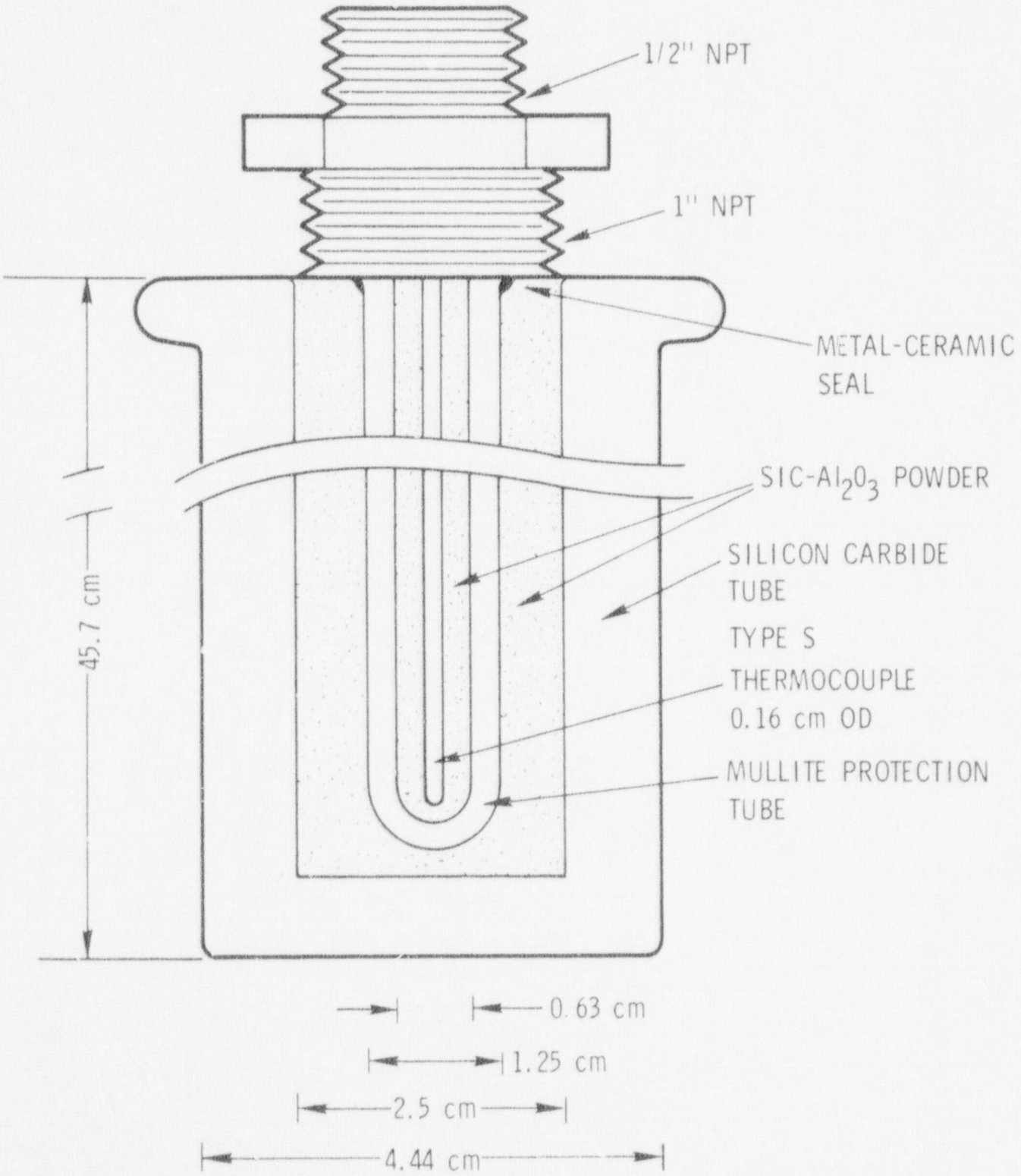

FIGURE 5. IN SITU THERMOCOUPLE ASSEMBLY.

The design of sensors to monitor the temperature of gases evolved during the test is shown in Figure 6. Type K thermocouples insulated with MgO and sheathed in a 0.16 cm OD 304 stainless steel tube were anchored in an array of 3 coaxial radiation shields. The radiation shields mitigate radiant heat losses from the warmed sensor to the cool surroundings. The flow-through design of the shields was intended to little distort convective heating of the sensor by the evolved gases. The innermost shield was a 0.63 cm OD, 0.47 cm ID type 304 stainless steel tube which also acted as a collar to stabilize the assembly in the gas stream. Other shields were made of 0.08 mm thick stainless steel shim stock and had diameters of 1.3 and 2.5 cm. The shields extended 12.7 cm along the thermocouple sheath so that conductive heat losses from the sensing junction were minimized.

Three gas phase thermocouples were located along a diameter of the crucible cavity at distances of 5.1, 7.6, and 19.0 cm from the nearest cavity wall. The sensing elements were suspended 11 cm above the top of the crucible.

Gas samples were collected from the stream evolved during the test in 150 cm^3 stainless steel bottles. The bottles were opened by remotely actuated Hoke, five way, ball valves. A vacuum pump connected to the sampling train allowed the bottles and connecting lines to be completely evacuated just prior to the test. Gas was drawn into the train through a 0.32 cm OD, 0.16 cm ID stainless steel tube whose internal volume did not exceed 1.3 cm^3. The tube was held over the center of the crucible cavity about 1.2 cm above the top of the crucible in a 1.9 cm OD steel pipe. A conical stainless steel flue 12 cm in diameter at its widest was mounted around the sampling tube to provide a gas stagnation point and reduce the ability of atmospheric gases to enter the port.

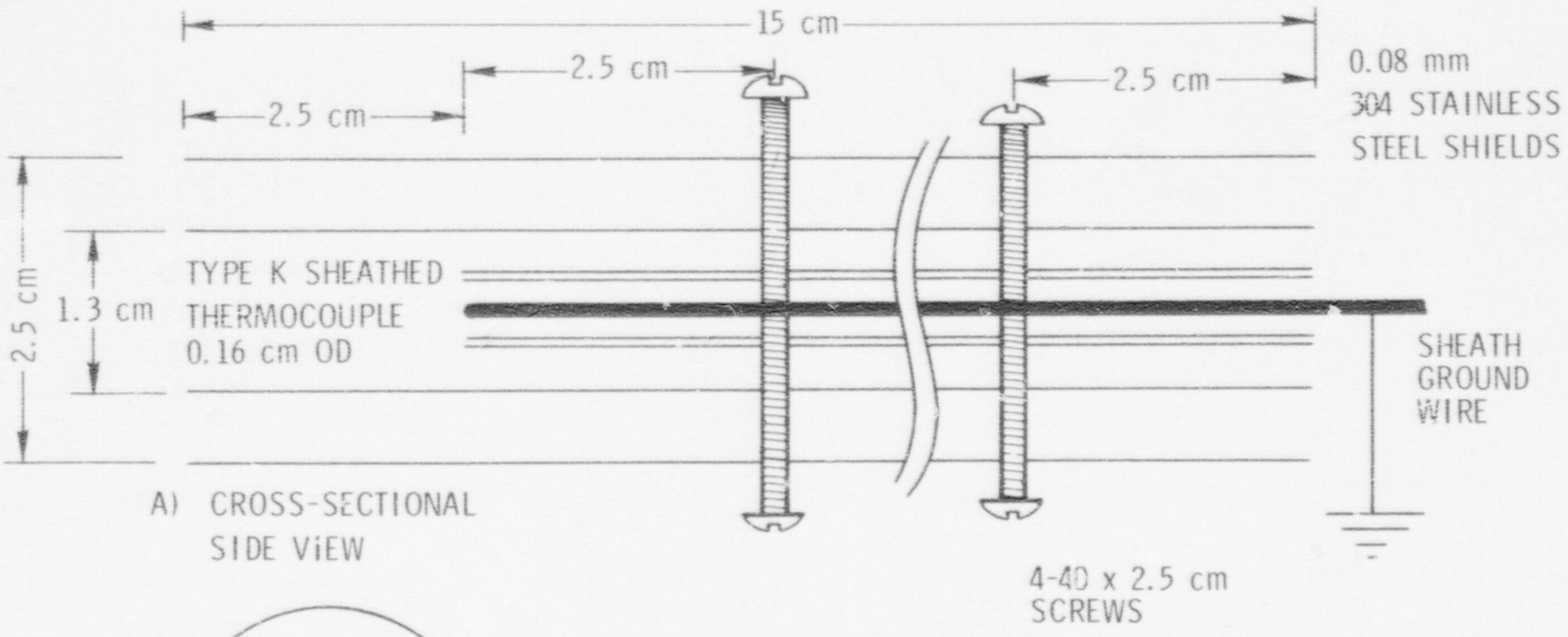

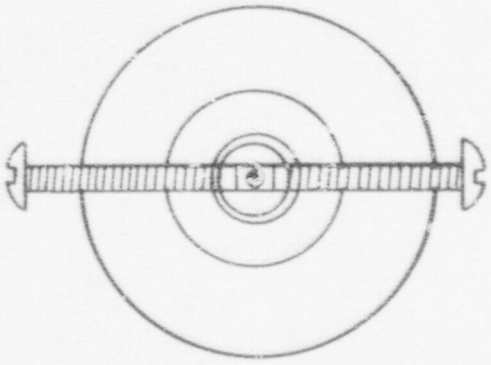

FIGURE 6. THERMOCOUPLE ASSEMBLY USED TO MONITOR GAS PHASE TEMPERATURE.

THERMOCOUPLE IS SHEATHED IN 304 STAINLESS STEEL.

THE INNERMOST SHIELD IS A STAINLESS STEEL TUBE 0.63 cm OD, 0.47 ID.

Sixteen type K, stainless steel sheathed, MgO insulated, 0.16 cm OD thermocouples were embedded in the concrete at various distances from the crucible cavity bottom. The thermocouples were mounted on two stations of eight thermocouples each. These stations, shown schematically in Figure 7, consisted of 10 cm diameter Lucite mounting rings affixed to a Lucite board attached to the bottom of the crucible. Thermocouples were symmetrically spaced on these rings so that gaps between sensors were 1-1/4 to 2 times the characteristic dimensions of the concrete aggregate. This spacing insured that concrete surrounding the sensors was representative of the bulk concrete. The sensing junction of the thermocouples were located in the cementitious phases of the concrete during crucible fabrication. These embedded thermocouples sense, then, the thermal behavior of these phases rather than the response of concrete aggregate or an average concrete thermal response. Spacing and locations of the thermocouples were maintained by three 8.9 cm diameter, 1.13 cm thick stainless steel rings located 3.8, 15.2 and 25.4 cm from the bottom of the crucible. A 5 cm hole in the various mounting and support rings of the thermocouple stations admitted a pipe used to further stabilize the thermocouples during the rougher stages of crucible manufacture.

One thermocouple station (labeled "C") was centered on the axis of the crucible cavity. The second station (labeled "R") was centered 14 cm to one side of this axis. Locations of the thermocouples on these stations, relative to the bottom of the crucible cavity, are listed in Table 4. The accuracies of these locations are about ± 0.3 cm.

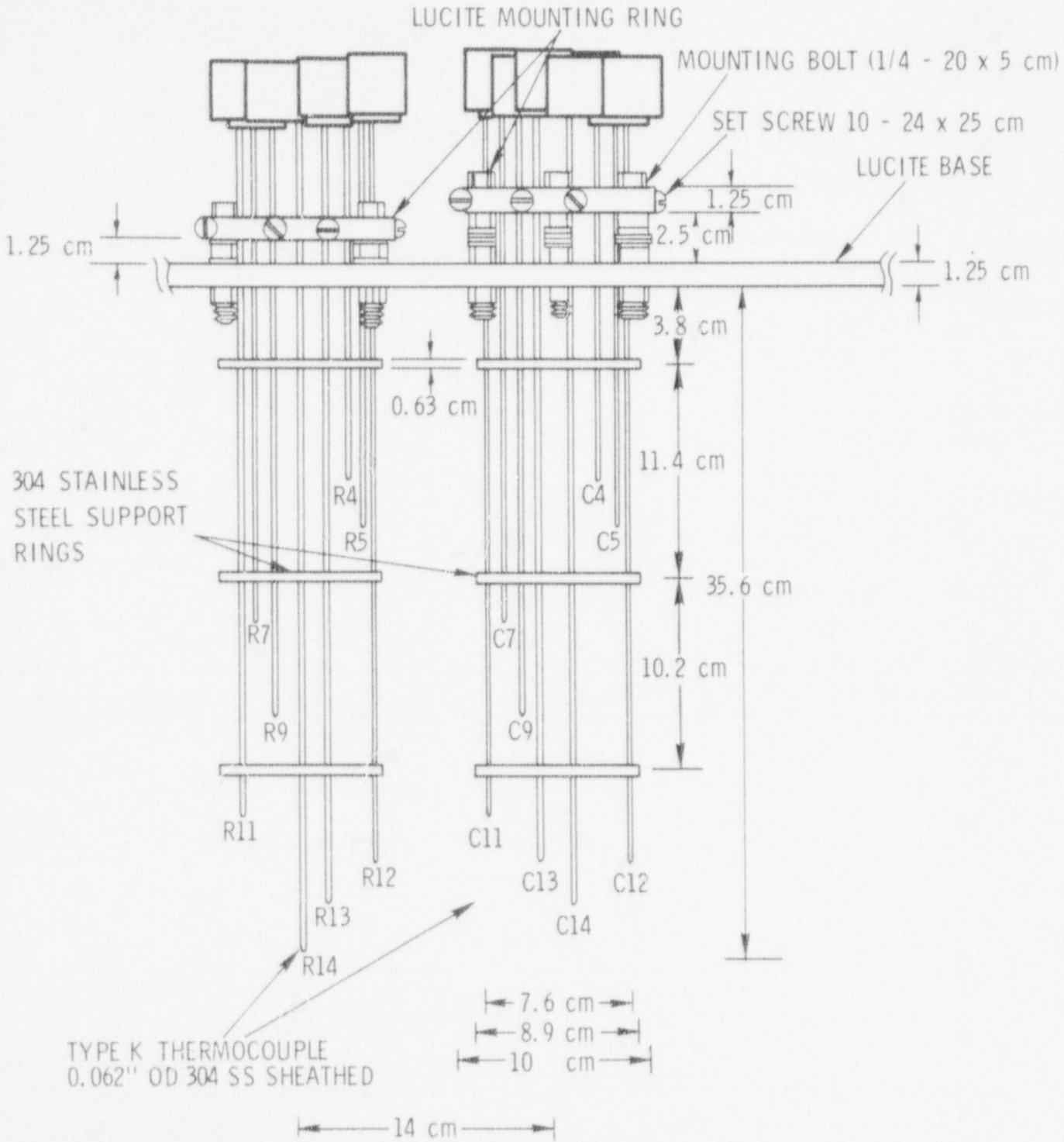

FIGURE 7. SCHEMATIC VIEW OF THERMOCOUPLE ASSEMBLIES USED IN THE FIXTURES FOR SUSTAINED MOLTEN STEEL-CONCRETE INTERACTIONS (Top View shown in Table 4).

TABLE 4

THERMOCOUPLE LOCATIONS IN THE FIXTURES FOR THE SUSTAINED TESTS OF MOLTEN STAINLESS STEEL - CONCRETE INTERATIONS

THERMOCOUPLE	DISTANCE FROM THE CAVITY SURFACE * in. (cm)
C14	0.0 (0.0)
C13	1.0 (2.5)
C12	2.0 (4.1)
C11	3.0 (7.6)
C9	5.0 (12.7)
C7	7.0 (17.8)
C5	9.0 (22.9)
C4	10.0 (25.4)
R14	0.0 (0.0)
R13	1.0 (2.5)
R12	2.0 (5.1)
R11	3.0 (7.6)
R9	5.0 (12.7)
R7	7.0 (17.8)
R5	9.0 (22.9)
R4	10.0 (25.4)

*Accuracy of Location = ± 0.12" (0.30 cm)

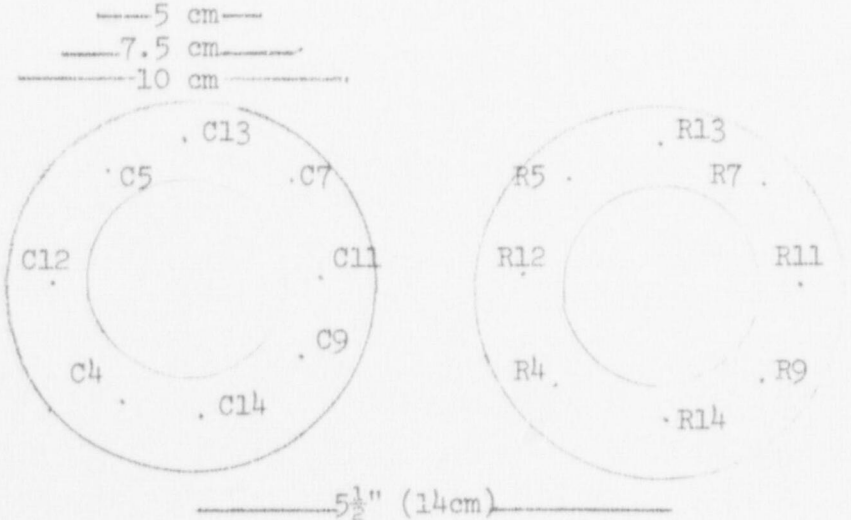

III RESULTS

Discussion is freely mingled with descriptions of the test results presented below in two sub-sections. The first sub-section consists of qualitative and subjective observations drawn from photographic records of the test and post-test inspection of the test fixture. Quantitative data obtained in the test are described in the second sub-section.

It must be emphasized again that these are preliminary results and caution should be exercised before they are used or extrapolated to other experimental situations.

A. QUALITATIVE RESULTS

Contact between the molten stainless steel and concrete initiated a vigorous pyrotechnic display that increased in intensity throughout the teem (see Figures 8 and 9). Flames, fully developed 0.58 seconds after the start of the metal pour, reached a maximum height of over nine feet shortly after the teem was complete. (See Figure 10). The flames were accompanied throughout the test by a dense, brown aerosol. Voluminous gas evolution early in the test caused harsh vibrations in instrumentation mounted above the crucible cavity. Vibration coupled with intense upward heat flux from the melt destroyed the stagnation flue on the gas sampling port and knocked radiation shields from two gas phase thermocouples. These fixtures had easily survived the environment created in similar, transient, melt/concrete interaction tests.

The vigor of the pyrotechnics and gas evolution early in test COIL-1 was apparently greater than that observed in similar transient tests. This intensity of early activity may be ascribed to use of a cylindrical crucible cavity in the sustained test rather than a hemispherical cavity as was used in the transient tests.

Ejection of substantial volumes of melt began shortly after the teem was complete (see Figure 11) and continued throughout the test. Ejected melt ignited some flammable material at the base of the crucible. Post-test examinations showed that of the 200 kg of metal originally teemed into the crucible only 101.8 kg remained as a coherent, solidified slug in the cavity. Much of the balance of the metal coated the walls of the cavity and the top of the crucible.

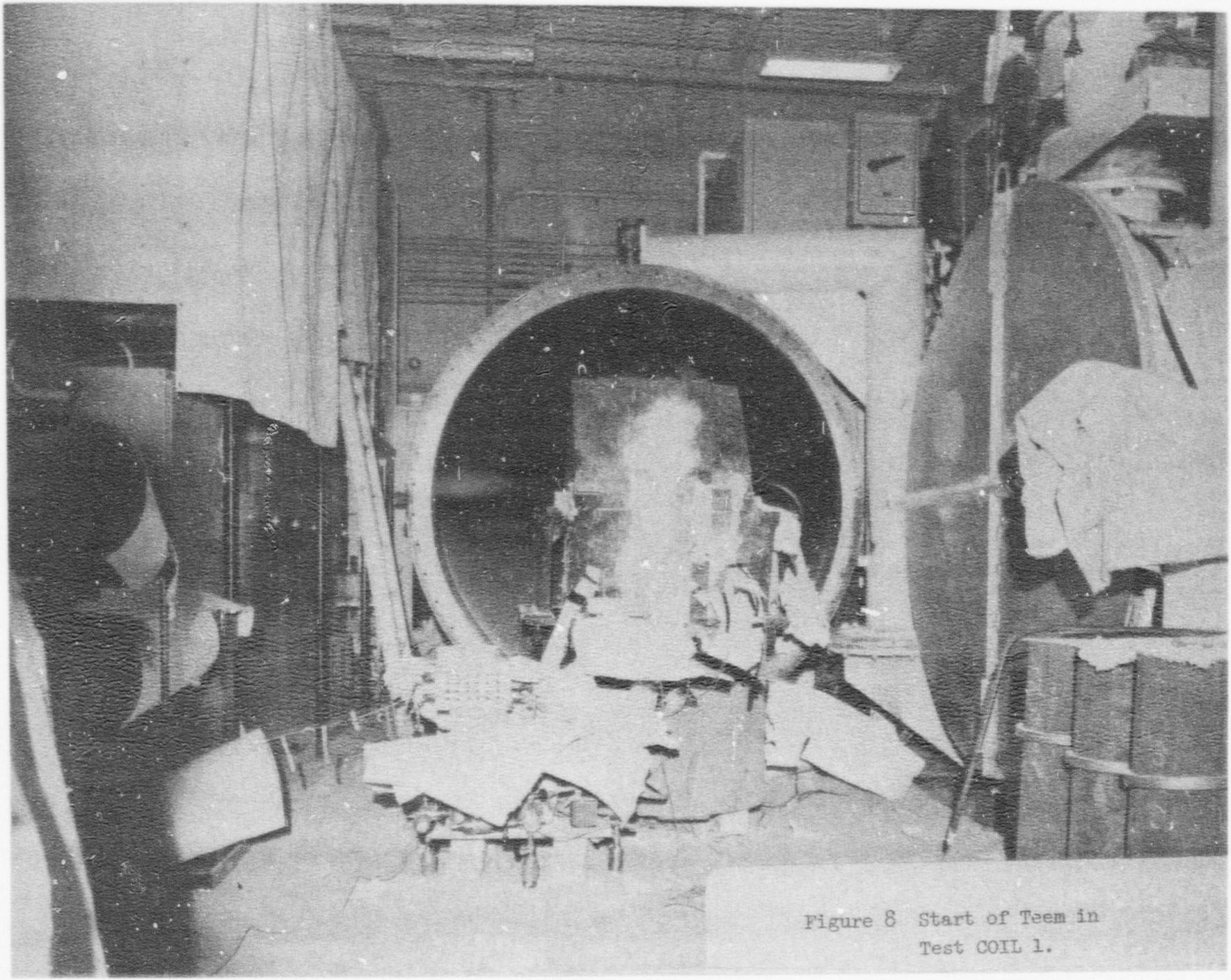

Figure 8 Start of Teem in Test COIL 1.

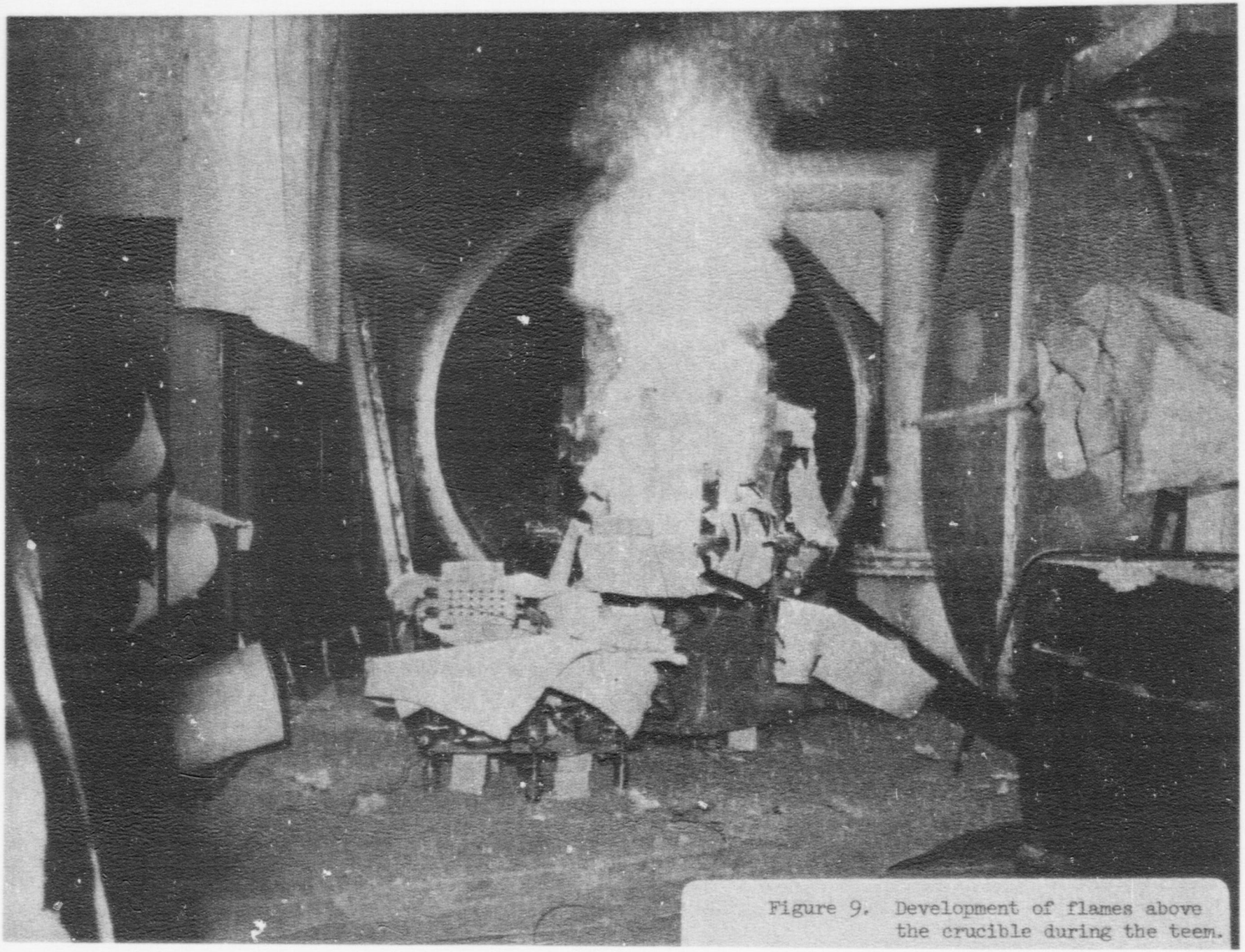

Figure 9. Development of flames above the crucible during the teem.

Figure 10. Flames reach their maximum height after the teem was complete and the furnace returned to its upright position.

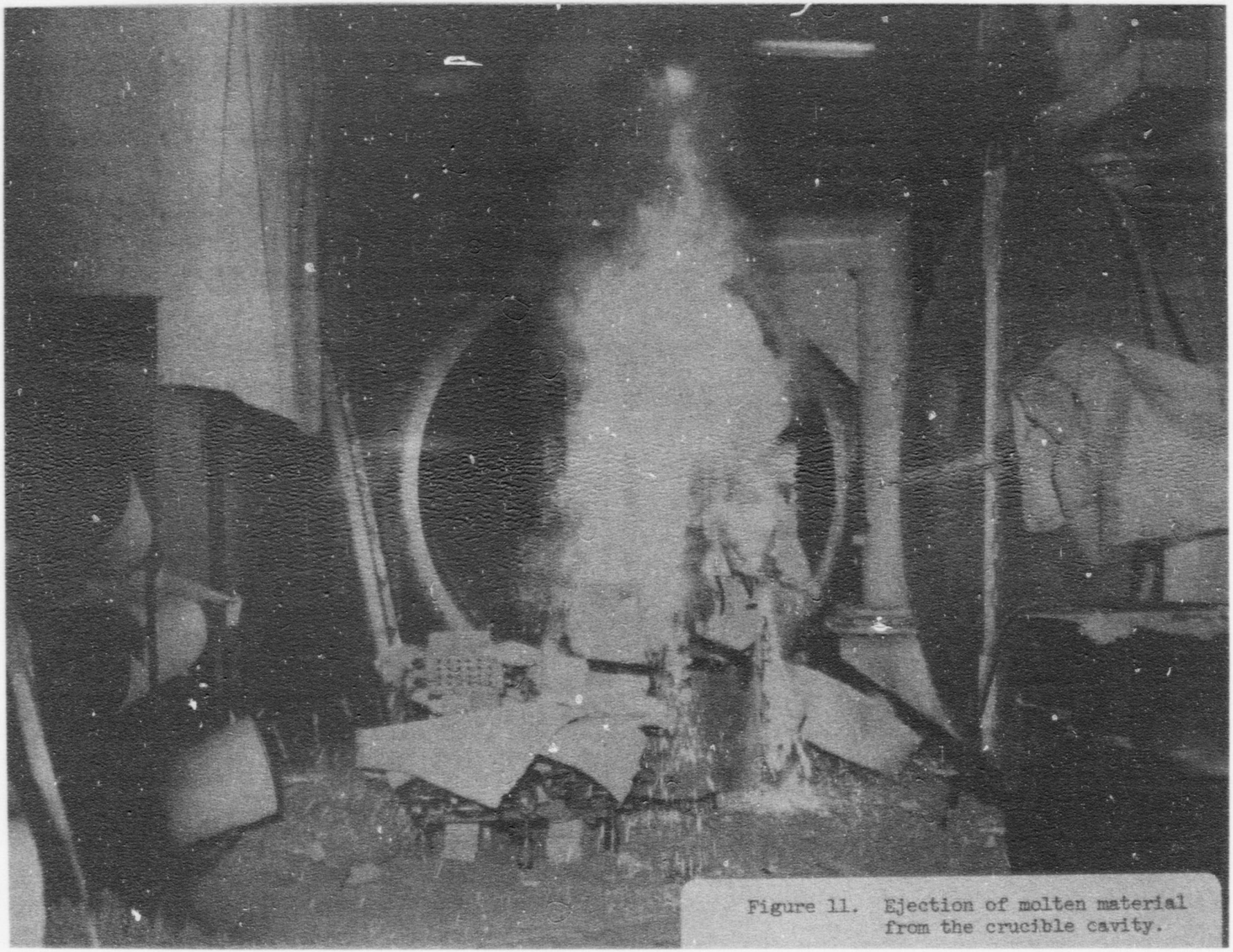

Figure 11. Ejection of molten material from the crucible cavity.

The flames and aerosols produced by the interaction waned during the test. This waning was interrupted by periodic pulsations whose frequency increased and magnitude decreased as the test progressed. Some of the pulsations were quite abrupt and were accompanied by ejection of metal from the experimental fixture (see Figure 12).

Flames produced during test COIL-1 were initially brilliant yellow. As the flames lost intensity they also assumed a blue tint. This caused some anxiety among the experimentors since blue flames are indicative of hydrogen burning. It was feared water might be accumulating under the melt either as a natural consequence of the melt/concrete interaction or because the embedded induction coil had been punctured. For this reason, the test site was abandoned when the sustained portion of the test was completed, and the natural cooling phase of the experiment COIL-1 was not observed.

Throughout the test the melt was kept vigorously agitated by escaping gases that had been thermally liberated from the concrete. Forced convection patterns produced in the melt by these gases were quite similar to those observed in transient tests ard appeared to overwhelm all other processes which might be expected to stir the liquid metal. No visual evidence of electromagnetic stirring could be seen either during the test or in photographic records of the test.

Flames, aerosol, and the intense radiant heat losses from the melt prevented close observation of the melt surface. During the first four minutes of the test it was not possible to ascertain if or how efficiently stratification of the melt into slag and metal layers had occurred. Later in the test a distinct slag layer could be seen. This layer was fairly liquid throughout the sustained portion of the test. Its behavior was not different than slag behavior observed in similar transient tests.

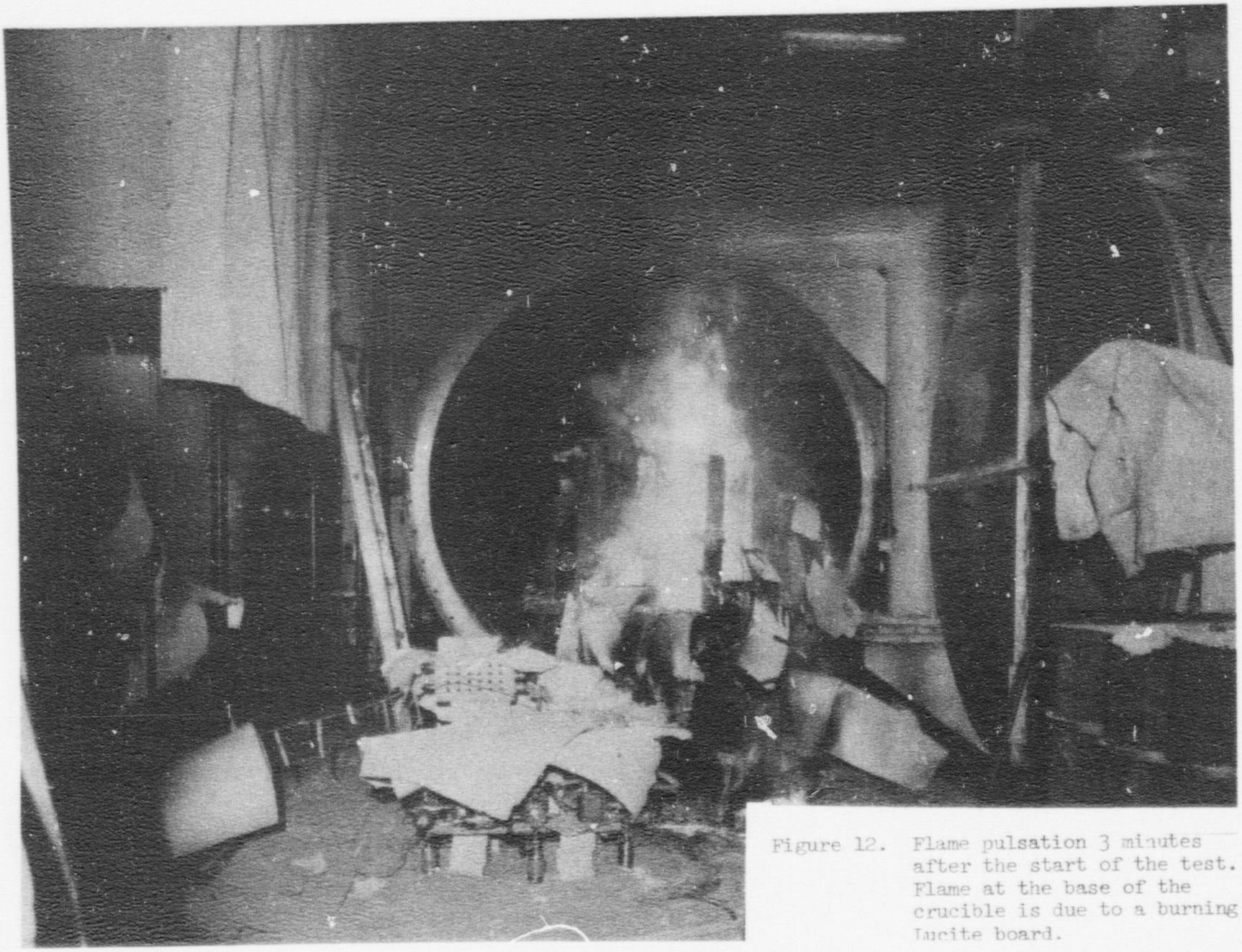

Figure 12. Flame pulsation 3 minutes after the start of the test. Flame at the base of the crucible is due to a burning Lucite board.

No concrete spallation was observed during the test. This result is entirely consistent with observations made in transient tests with similar melts and concrete.

The concrete crucible sustained major horizontal cracks even with the top of the embedded induction coil. This portion of the crucible was not reinforced. It was particularly weak since it contained fireclay blocks used to support the induction coil during fabrication of the test fixture. The horizontal cracks passed completely through the crucible wall and large concrete pieces could be readily pulled from the top of the crucible at the end of the test (see Figure 13a). These horizontal cracks were above the molten pool during the test and liquid had not entered the fissures.

Some vertical cracks were observed in the lower portion of the crucible which was reinforced by the induction coil. These cracks were not sufficiently developed to cause any significant loss of structural integrity in the lower portion of the crucible.

Water migration to the external walls of the crucible was not observed in test COIL-1. Post-test examination of the test fixture revealed that asbestos paper lining the induction coil was saturated with water. Water migration within the concrete was apparently halted at the cool boundary established in the crucible by the induction coil. Temperature of the cooling water in the coil did not exceed 41°C during the test.

The solidified metal slug was wedged tightly into the crucible, but had not bonded to nor wetted the concrete. The upper surface of the slug was coated with a dense, dark-brown slag which was no more than 1 cm thick except where the fireclay block used to locate the *in situ* melt thermocouple had floated to the surface (see Figure 13b). Metal near the surface of the solidified slug appeared to be badly oxidized.

FIGURE 13 - POST TEST PHOTOGRAPHS OF THE CRUCIBLE

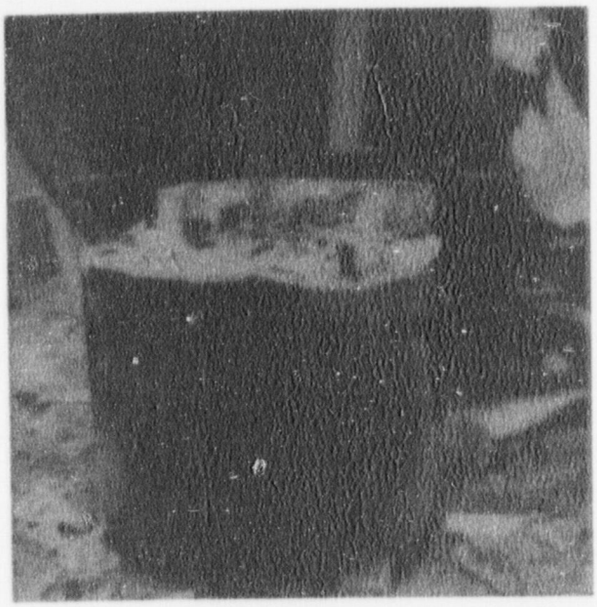

(a) Plane of cracking in the crucible after the loose concrete had been removed.

(b) Top view of the partially removed metal slug

Sectioning of the slug showed it to be of compact metal. Near the top surface voids and inclusions were noticeable, some of which passed a few centimeters into the slug (see Figure 14).

The concrete underlying the solidified metal slug was a white or yellowish powder which was obviously the product of considerable thermal alteration of concrete. No distinct incipient melt zone was present.

Erosion profiles of the crucible have not been made to date. Erosion was predominately downward. The erosion amounted to about 10 cm at the center of the crucible. The extent of erosion decreased toward the walls of the crucible so that the bottom of the cavity had an approximately dish-shaped or conical appearance. Radial erosion of the cavity walls was fairly insignificant. The diameter of the crucible was increased during the test by no more than 1.5 cm.

The limited radial erosion of the concrete is not believed to be due to the presence of the water-cooled induction coil. The geometry of the crucible cavity should lead to enhanced gas generation near its perimeter. Gases passing up the walls of the cavity, being of greater volume than gases generated at the bottom, shield the walls from attack by the metal and reduce the rate of erosion on the walls relative to that at the bottom of the cavity. Circulation of the melt induced by the gases rising in this manner would also provide a rationalization of the post-test cavity shape.

B. QUANTITATIVE RESULTS

Pyrometric data from the test is plotted in Figure 15 as brightness temperature versus time. It is unclear whether the energy received by the pyrometer detector came from melt or flame

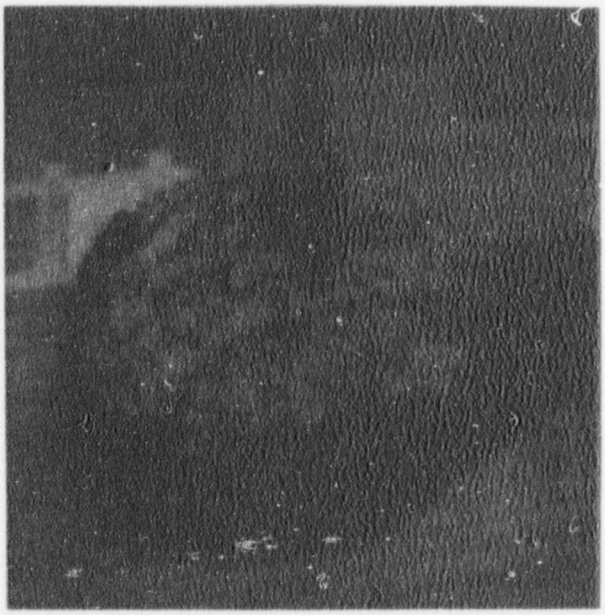

a) Bottom of metal slug after it has been sectioned

b) Side view of the slug

Figure 14 Post-Test Photographs of Solidified Metal from Test Coil-1

Figure 14 cont'd.

c) Side view showing interior of slug. Note voids at the top and compact metal near the bottom of the slug

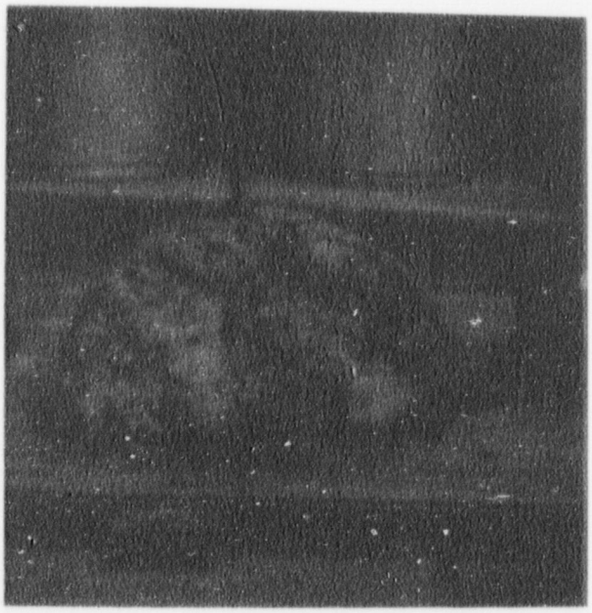

d) Top view of the slug

emissions. The shape of the temperature-time curve in Figure 15 does not mimic well the shapes of similar curves produced by the gas phase temperature sensors (see Figure 20). Under the assumption that the melt temperature was being monitored by the pyrometer, the maximum observed brightness temperature (1656°C) was set equal to the known melt temperature at the start of the test (1720°C) and an emissivity value determined. The derived value, 0.87, agrees well with the literature value, 0.85, reported for oxidized 18-8 stainless steel (11). The brightness temperatures, corrected for emissivity effects, are also shown in Figure 15. At best these corrected results describe the temperature of the melt surface, which is likely to be the coolest part of the melt.

After about 60 seconds, output from the pyrometer dropped sharply, though flames above the melt cavity were still fairly bright and the temperature of the melt was still quite high at this point in the test. Melt expulsion from the crucible and concrete erosion may have combined to substantially reduce the level of melt in the crucible cavity--possibly below the line-of-sight of the pyrometer.

The in situ melt thermocouple was failed by mechanical stresses which exposed the sensor to the melt early in the test. What little data this sensor did yield are shown in Figure 16. Failure obviously occurred before the massively shielded thermocouple could come into thermal equilibrium with the melt.

Three melt temperature measurements were made with immersion thermocouples at 360, 480 and 540 seconds after the start of the test. Temperatures at these times were 1508, 1502, and 1487 $\pm$ 5°C, respectively.

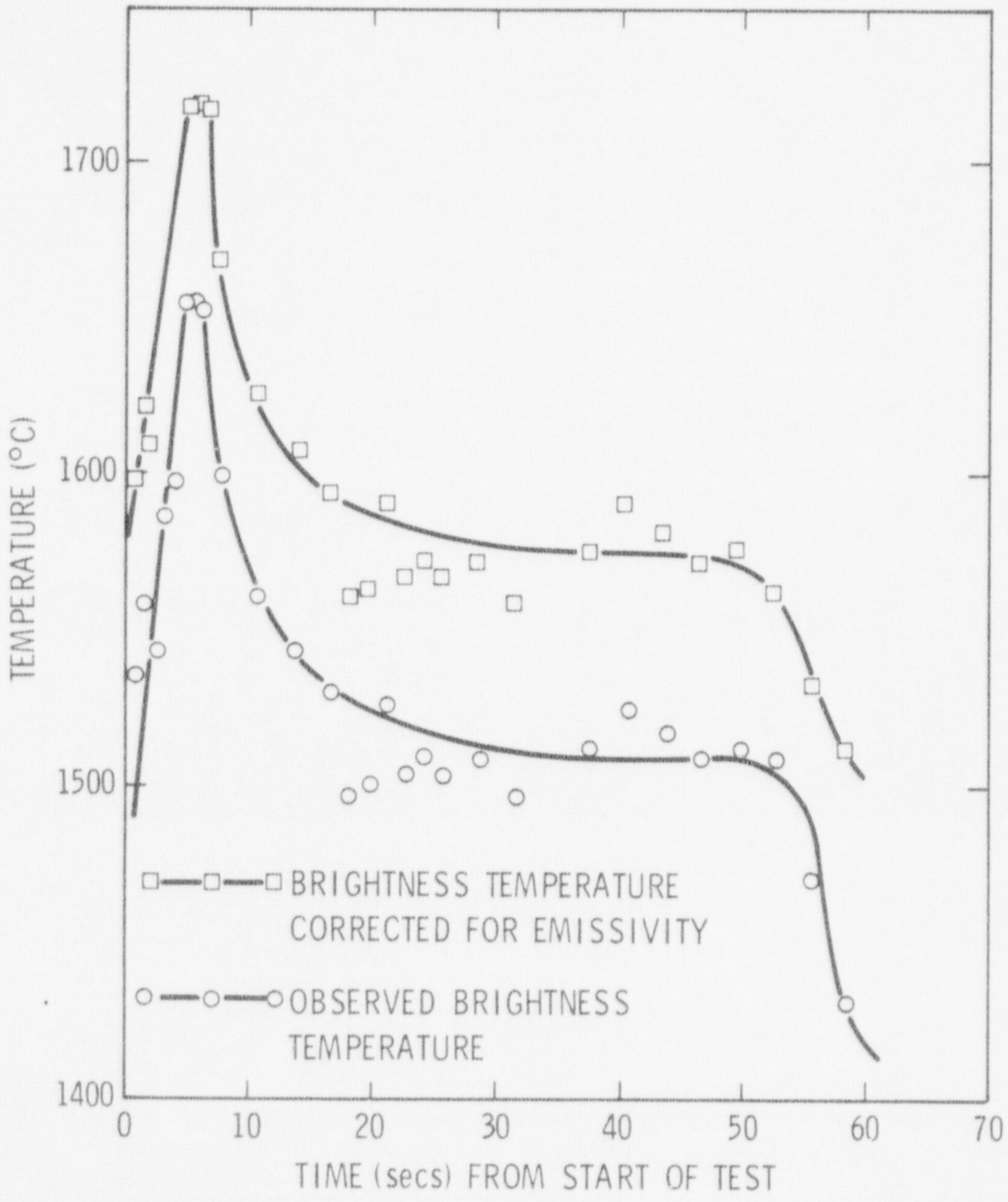

FIGURE 15. MELT TEMPERATURE DATA FROM PYROMETER OBSERVATION IN TEST COIL-1 VERSUS TIME.

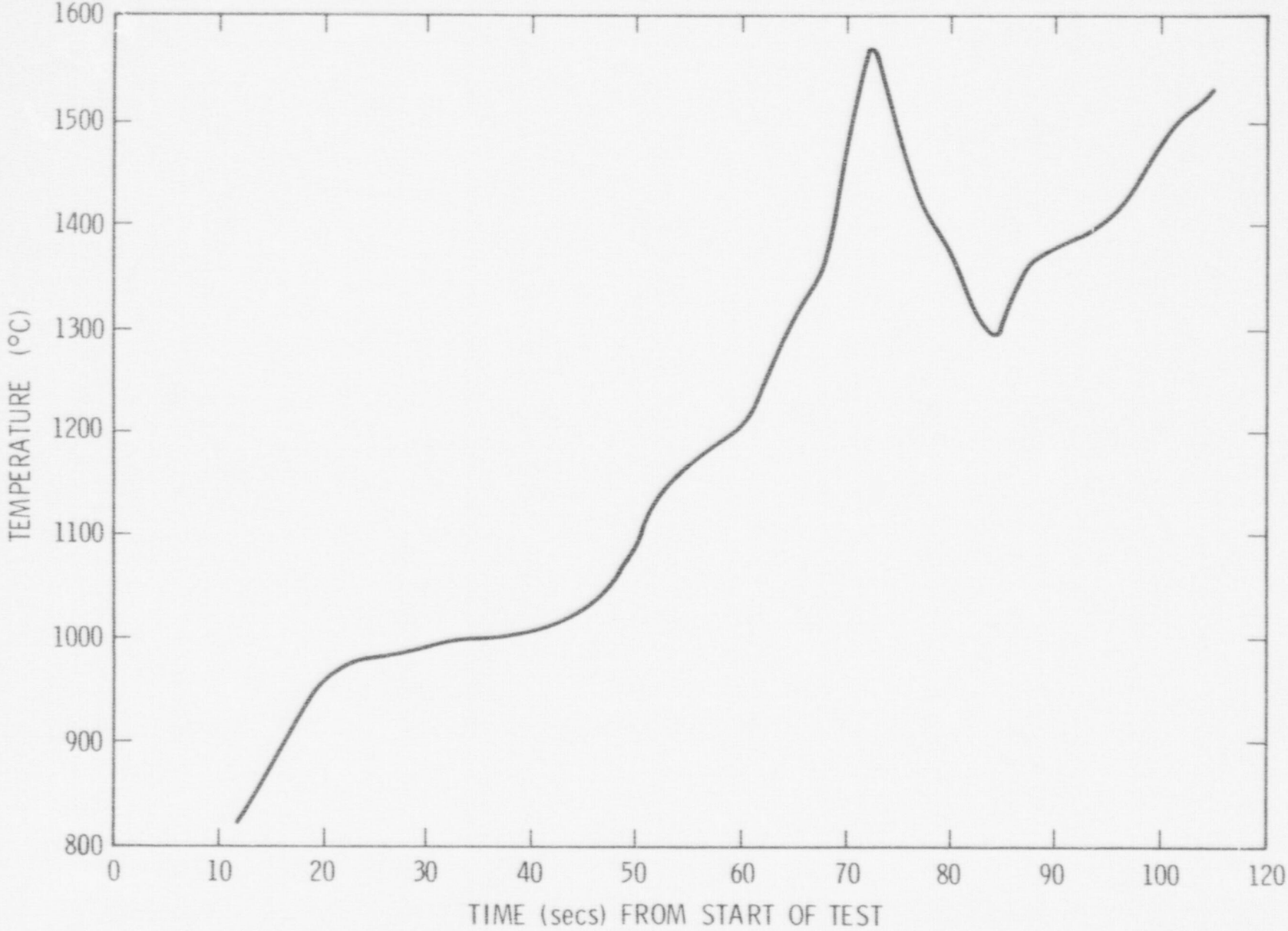

FIGURE 16. OUTPUT FROM IN SITU THERMOCOUPLE IN TEST COIL-1 VERSUS TIME.

These temperatures are plotted in Figure 17 along with melt temperature data from a similar, though transient, test with a melt and concrete identical to that used in test COIL-1. Cooling in the transient test is arrested at about 1460°C where solidification of the melt begins and the heat of crystallization makes up for heat losses from the melt. Cooling in test COIL-1 was arrested at about 1500°C where heat input from the induction coil balances heat losses from the melt. Electrical coupling between the melt and the coil was not sufficient to maintain temperatures above the liquidus of the concrete. The sustained temperature was greater than the solidus temperature of this particular variety of concrete.

Compositions of gas samples collected during the test are listed in Table 5. The compositions of these samples have been recalculated ignoring atmospheric gases (O_2, N_2, and Ar) which were either drawn along with the samples or were entrapped in the gas sampling train. These contaminating gases sometimes amounted to 20 volume percent of the sample, but were usually less than 10 v/o. Past experiences with gas samples of this type have shown that their compositions are consistent with gas mixtures quenched from equilibrium at 700 to 800°C. Gases are, of course, drawn into the sampling apparatus at much higher temperatures. The gases maintain chemical equilibrium as they cool until they reach the above temperature range. Thermodynamic analysis of the results is necessary if the gas compositions at the sampling temperatures are to be reconstructed. Past experience with similar samples suggests that the carbon monoxide concentration of the mixture would increase at the expense of the carbon dioxide content and the water concentration would increase at the expense of the hydrogen concentration as temperature increases. (11) That is, the equilibrium

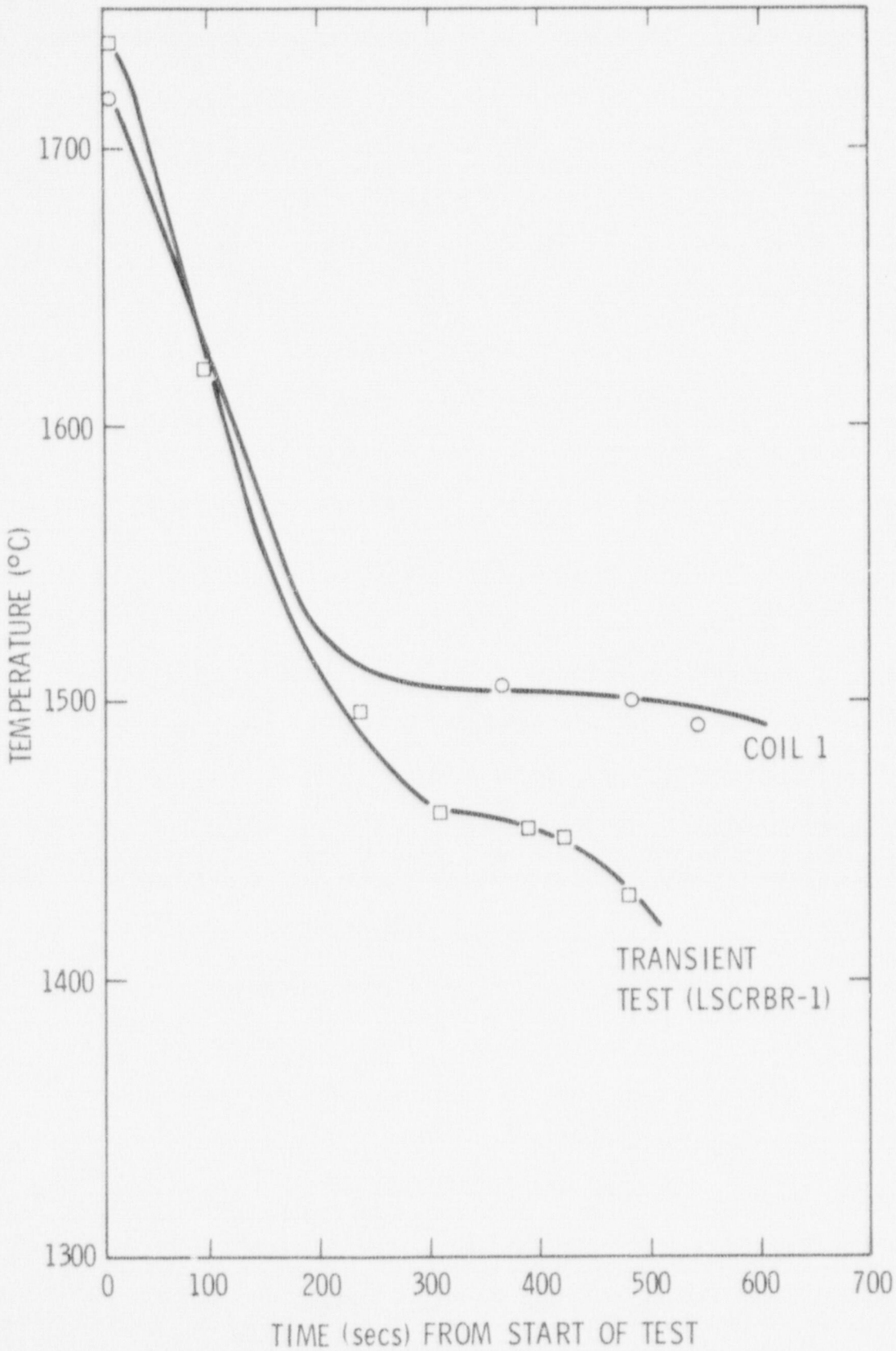

FIGURE 17. MELT TEMPERATURE DATA OBTAINED WITH IMMERSION THERMOCOUPLES IN TEST COIL-1 AND A SIMILAR TRANSIENT MELT/CONCRETE INTERACTION TEST.

TABLE 5

COMPOSITIONS OF GAS SAMPLES FROM TEST COIL-1

Time (secs)[a]	Volume % H_2	CO	CO_2	CH_4	C_2H_4	C_2H_6	H_2/C[c]
18	36.0	53.0	10.8	0.19	-	-	0.568
23	47.8	46.6	5.6	tr[b]	-	-	0.916
28	60.8	35.1	4.1	tr[b]	-	-	1.55
136	35.5	43.5	20.9	-	-	-	0.551
199	20.8	62.2	17.1	tr[b]	-	-	0.262
204	tr[b]	90.6	7.5	1.87	tr[b]	-	0.037
267	31.1	57.4	2.3	6.37	2.88	tr[b]	0.690
272	70.7	20.1	0.9	5.91	2.37	-	2.76
335	39.0	29.9	2.1	20.6	8.24	tr[b]	1.59
340	68.9	13.0	1.4	12.2	4.60	tr[b]	2.86
403	38.7	26.4	2.8	23.1	8.92	tr[b]	1.46
408	42.9	19.7	2.5	25.1	9.79	tr[b]	1.68

(a) Seconds from start of metal teem
(b) trace; less than 500 ppm by volume
(c) effective molar ratio of hydrogen content of gas from all chemical species to the carbon content of gas from all chemical species

$$CO + H_2O \rightleftharpoons CO_2 + H_2$$

shifts to the left with increasing temperature.

The compositions of the gas samples fluctuate widely over the course of the test. Such behavior may be characteristic of the melt/concrete interaction, or it may reflect the close proximity of the sampling port to the melt surface where the discontinuous nature of gas evolution could be sensed. Consistent trends in the nature of the evolved gas are difficult to detect.

The molar ratios of hydrogen to carbon from all constituents in the gas mixtures are plotted versus time in Figure 18. In all cases, save two, these ratios are greater than the H_2/C ratio in the concrete. The disparity between the gas and concrete H_2/C ratios is believed to be a consequence of the nature of heat transfer from the melt into the concrete. Thermal alteration of concrete to yield gaseous species does not occur at the melt/concrete interface except at the very start of the interaction. Once surface concrete material is destroyed, further gas generation occurs below the melt/concrete interface at depths dictated by the temperature profile in the concrete. Dehydration of concrete is essentially complete at 500°C. Decarboxylation of the concrete is not significant until temperatures in excess of 600°C are reached. The gas data suggest that the lower temperature dehydration front penetrates into the concrete more rapidly than does the decarboxylation front. In a sufficiently prolonged melt/concrete interaction the H_2/C ratio would eventually fall to zero when dehydration of the concrete was complete. This hypothesis is consistent with previous experiments dealing with heat-transfer in concrete (13).

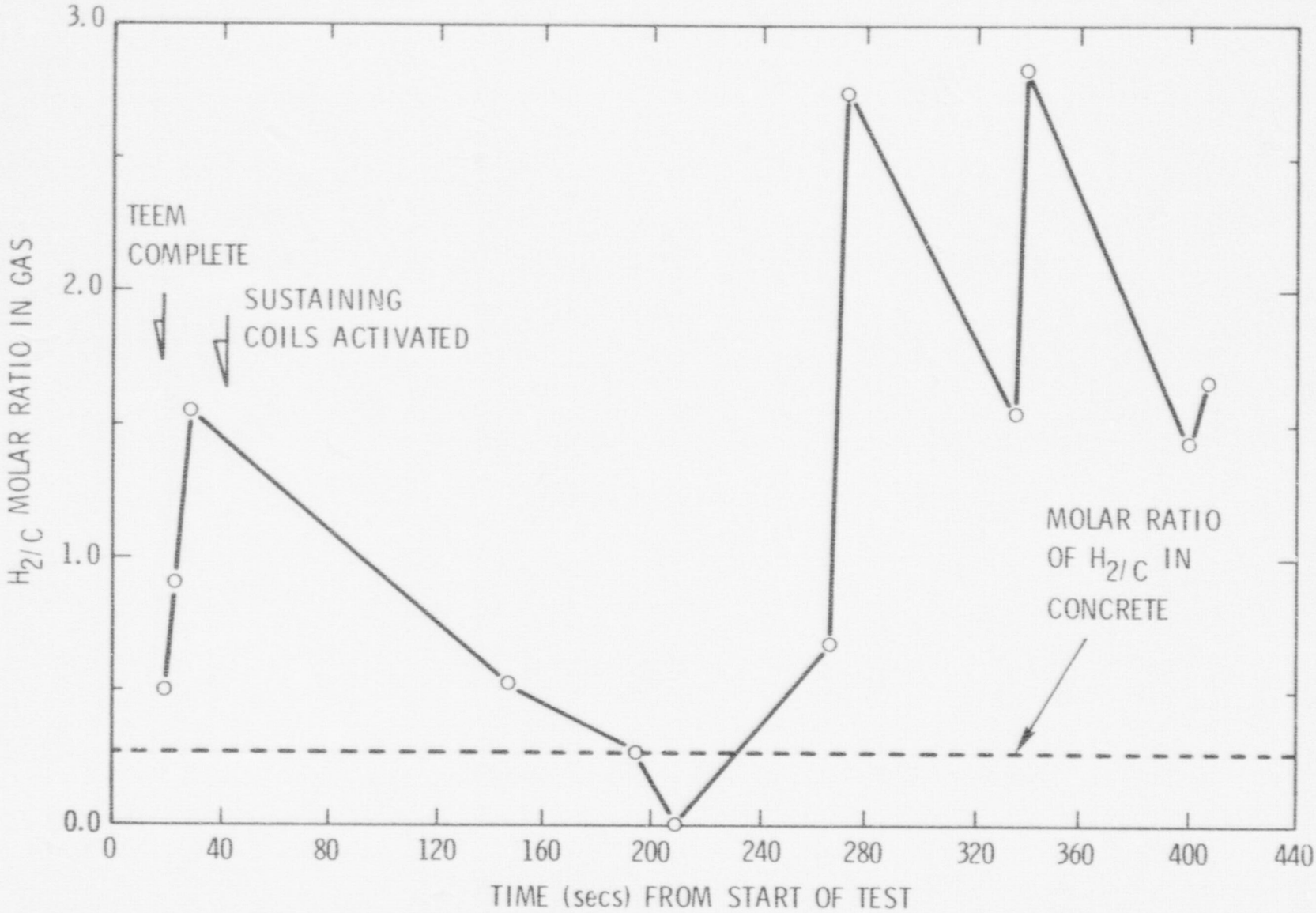

FIGURE 18. MOLAR RATIO OF H_2/C IN GAS STREAM PRODUCED IN TEST COIL-1 VERSUS TIME.

Methane, ethene and even traces of ethane appear in the gas samples three minutes after the start of the test. As shown in Figure 19, the concentrations of methane and ethene increase with time eventually reaching maximum values of about 25 and 10 volume percent, respectively.

The hydrocarbon constituents of the gas are surprising since hydrogenation reactions such as

$$CO + 3H_2 \rightarrow CH_4 + H_2O$$

and

$$2CO + 4H_2 \rightarrow C_2H_4 + 2H_2O$$

do not proceed significantly to the right at temperatures encountered in the melt. The hydrocarbons must, therefore, be the products of reactions in the gas phase once it has cooled somewhat. Hydrogenation of carbon monoxide is typically kinetically slow because of the strength of the carbon to oxygen bond. The observed concentrations of hydrocarbons in the gas stream suggest that the speciation of the gas has benefited from catalytic assistance. Nickel, available in quenched portions of the melt about the orifice of the crucible cavity and in the stainless steel gas sampling probe, is an effective catalyst for hydrogenation of carbon monoxide.

It is likely that catalytic activity of the gas sampling probe was responsible for the hydrocarbons. The gas sampling probe used in the experiment was located close to the orifice of the crucible cavity where it could be heated by the melt. The gas sampling line could easily have reached temperatures at which hydrogenation reactions proceed rapidly with catalytic aid and the products are thermodynamically stable. As the test proceeded a greater length of sampling line could have been heated to this temperature range. This would give sampled gas

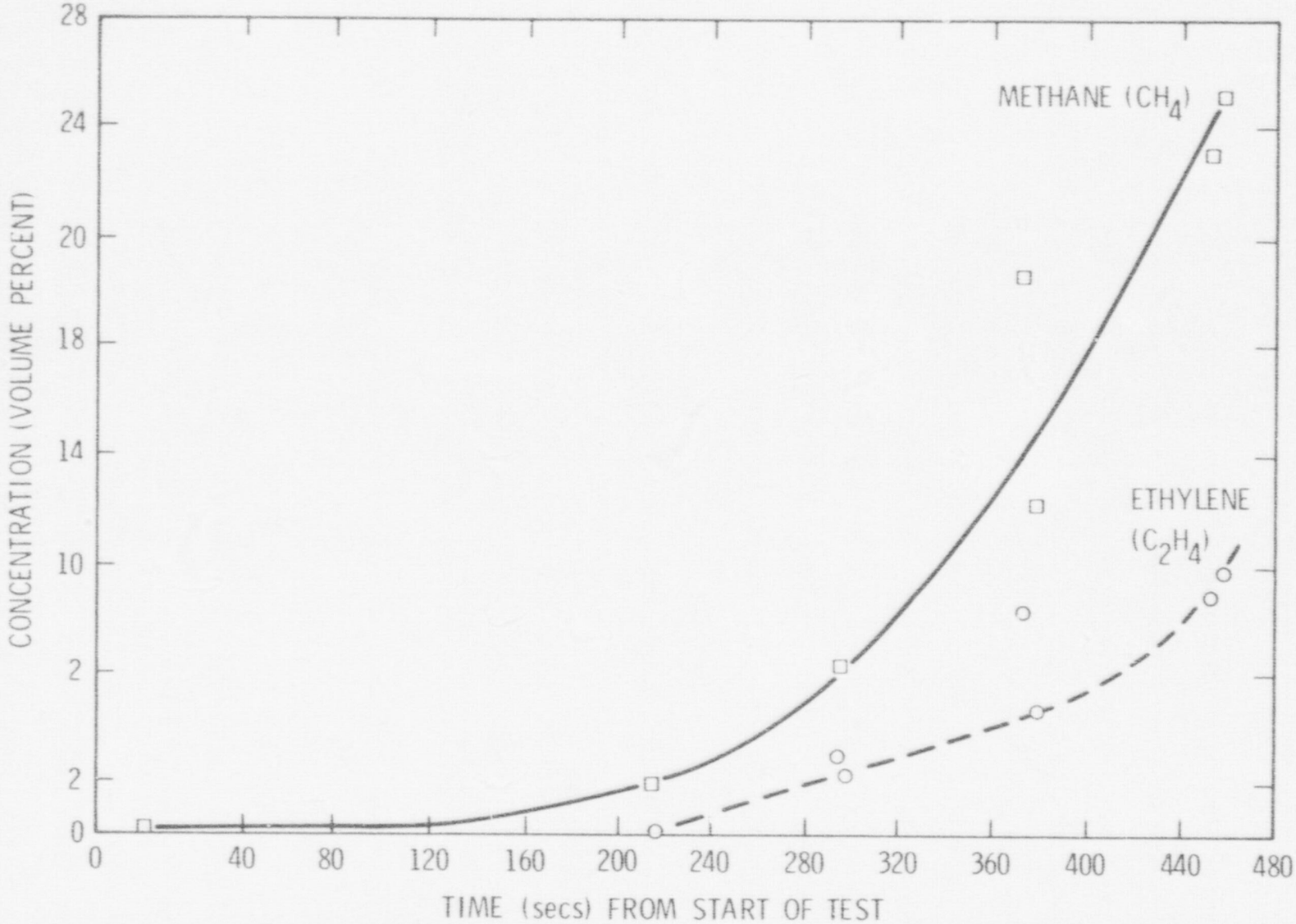

FIGURE 19. HYDROCARBON CONCENTRATION IN GASES SAMPLED DURING TEST COIL-1 VERSUS TIME FROM THE START OF THE TEST.

greater contact time with the catalyst. Such behavior would explain both the appearance of hydrocarbons in the gases and qualitatively the time dependencies of their concentrations.

Gas phase temperatures are plotted versus time in Figure 20. Asterisks in these plots mark the times at which radiation shields on two of the thermocouples were knocked from the sensors. Thermocouples located 7.6 and 19.0 cm from the perimeter of the crucible cavity behaved quite similarly. The thermocouples 5.1 cm from the cavity perimeter registered much lower temperatures early in the test. Six minutes after the start of the test, readings from the three sensors were all quite similar.

Gas temperature data suggest that the upward heat-flux from the melt falls dramatically near the perimeter of the crucible cavity. Such spatial dependence of the heat flux would be consistent with arguments concerning gas evolution made to rationalize the directional nature of concrete erosion. The data can also be explained in terms of cool ambient air being drawn into the stream of hot gases evolved during the melt/concrete interaction.

IV SUMMARY

All qualitative and quantitative results collected in this test indicate that inductive heating can be used to maintain large stainless steel melts in the liquid state while they are in contact with concrete. Electrical coupling between the induction coil and the melt was not sufficiently strong in test COIL-1 to maintain the melt at temperatures above the liquidus of the particular variety of concrete used in the experiment. Degradation of the coupling may have been due to metal expulsion from the crucible or to metal oxidation. Metal ejection can be controlled by making suitable modifications to the experimental apparatus.

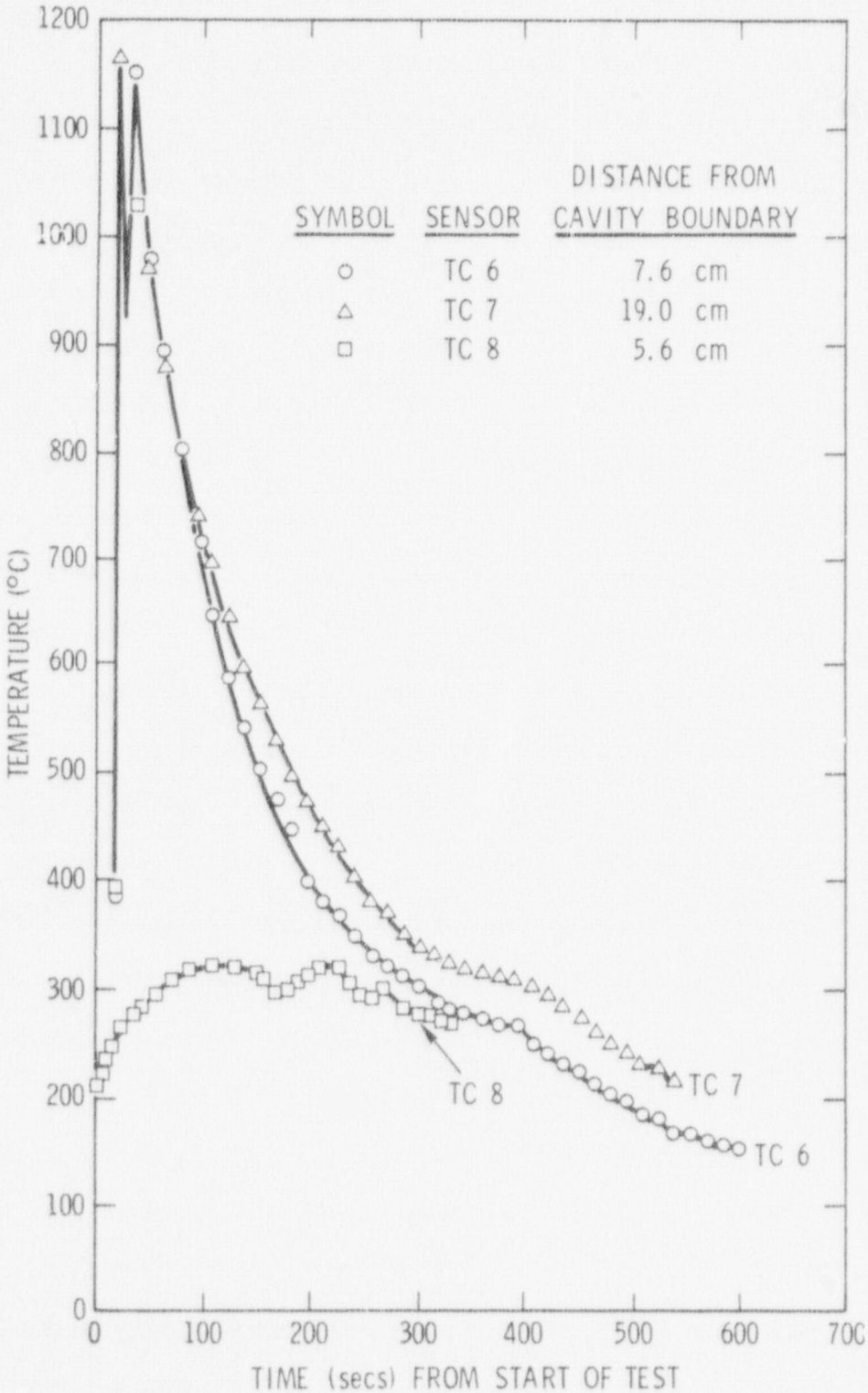

FIGURE 20. GAS PHASE TEMPERATURES IN TEST COIL-1 VERSUS TIME.

Metal oxidation, on the other hand, is innate to the melt/concrete interaction and is, in fact, an important phenomenon to be studied in experiments of this type. It cannot and ought not be controlled.

Post-test inspection of the test fixture showed that termination of test COIL-1 was brought about by a false alarm from the ground-fault detection system built around the induction coil. Current flow in the detection system may have been made possible by a variety of means such as short circuits created by metal expelled from the crucible or water migrating into the vicinity of the probes. In any case, it was not produced by the melt penetrating dangerously close to the water-cooled induction coil. The limited extent of radial erosion of the concrete by the melt suggests that experiments in which melt is sustained for at least 30 minutes are entirely feasible.

Test COIL-1 has also experimentally demonstrated that electrical instrumentation, including thermocouples, can be successfully used around an unshielded, high-power, induction coil. The thermal environment created in a sustained test, an environment far harsher than that generated in a transient melt/concrete interaction test, requires that sensing elements associated with the instrumentation be robustly shielded.

Instrumentation successfully used in test COIL-1 included monitors of gas temperature, concrete temperature, gas composition, and to a more limited state of proficiency melt temperature monitors. Melt temperature remains one of the most important and most difficult measurements to be made in a melt/concrete interactions tests. Experience gained in test COIL-1 with immersion, in situ and pyrometric monitors of melt temperature suggests that an in situ thermocouple may be successfully used provided it is located in the melt after the melt is deposited in the

test fixture. While appropriate materials selection can provide defense against the hostile chemical and thermal shock environment presented by the melt, mechanical stresses on the temperature probe must be avoided.

In addition to providing a demonstration of the utility of experimental techniques, test COIL-1 has yielded data concerning the nature of the melt/concrete interaction. The following points are demonstrated or suggested by the test results:

(a) gas generation by thermal decomposition of the concrete takes place below the melt/concrete interface in such a way that the gas composition does not reflect the composition of the eroding concrete,

(b) gases are reduced as they percolate up through the melt and the reduced gases may react to yield hydrocarbons such as methane, ethene, and ethane,

(c) gases produced in the test have a significant impact on the directional nature of concrete erosion by the melt,

(d) concrete spallation is not a significant aspect of concrete erosion by a metallic melt,

(e) upward heat transfer from the melt is a significant source of heat loss from the melt.

ACKNOWLEDGEMENTS: The author wishes to thank F. E. Arellano, A. F. Turbett, R. W. Fisher, F. M. Hosking, and N. Zamora for their assistance in this experimental work. The author especially thanks Dr. F. J. Zanner for his helpful suggestions and assistance in all aspects of this study. This project was funded by the Experimental Fast Reactor Safety Branch of the U. S. Nuclear Regulatory Commission.

REFERENCES

1) D. A. Powers, "Interactions Between Molten Nuclear Reactor Core Materials and Structural Concrete", International Colloquium on Chemical Reactivity at High Temperatures, Odeillo, France, June, 1977.

2) D. A. Powers, Molten Core-Concrete Interactions Program Description 189A No. A1019, Sandia Laboratories, Albuquerque, NM, Oct. 1975 Available from U.S. Nuclear Regulatory Commission.

3) D. A. Dahlgren et al, "Molten LWR Core Material Interactions with Water and with Concrete", Topical Meeting, Thermal Reactor Safety, Sun Valley, Idaho, July 31-August 4, 1977.

4) D. A. Powers, "Large-Scale Melt/Concrete Interactions Tests", Transaction Amer. Nucl. Soc., Volume 26 (1977), p. 400.

5) Light Water Reactor Safety Research Program Quarterly Report January-March 1976, SAND76-0369, Sandia Laboratories, Albuquerque, NM, September, 1976.

6) Light Water Reactor Safety Research Program Quarterly Report April-June 1976, SAND76-0677, Sandia Laboratories, Albuquerque, NM, February, 1977.

7) J. F. Muir, D. A. Powers, and D. A. Dahlgren, "Studies on Molten Fuel-Concrete Interactions", Proc. Int'l. Meeting on Fast Reactor Safety and Related Physics, Chicago, Illinois, Oct., 1976, CONF-761001 Volume IV.

8) W. B. Murfin, A Preliminary Model for Core/Concrete Interactions, SAND77-0370, Sandia Laboratories, Albuquerque, NM, July, 1977.

9) "Concrete Design Mixes", Clinch River Breeder Reactor Plant Technical Specifications 3066-10-6, Breeder Reactor Division Burns and Roe, Inc., August, 1976.

10) W. R. Bandi and G. Krapf, Thermochimica Acta 14 (1976) 221.

11) Handbook of Chemistry and Physics, 45th edition, Chemical Rubber Co., 1964.

12) Light Water Reactor Safety Research Program Quarterly Report October-December 1976, SAND77-0944, Sandia Laboratories, Albuquerque, NM, July, 1977.

13) J. F. Muir, Response of Concrete Exposed to a High Heat Flux on One Surface, SAND77-1467, Sandia Laboratories, Albuquerque, NM, November 1977.

DISTRIBUTION:

U. S. Nuclear Regulatory Commission
(R3, 356 copies)
Division of Document Control
Distribution Services Branch
7920 Norfolk Ave.
Bethesda, MD 20014

Dr. M. Fisher
Gesellschaft fur Kernforschung
Project Nuclear Safety (PNS)
75 Karlsruhe
Postfach 3640
Federal Republic of Germany

Dr. H. Holleck
Gesellschaft fur Kernforschung
PNS/IMF
75 Karlsruhe
Postfach 3640
Federal Republic of Germany

Dr. H. Albrecht
Gesellschaft fur Kernforschung
PNS/IRCH
75 Karlsruhe
Postfach 3640
Federal Republic of Germany

Dr. J. P. Hosemann
Gesellschaft fur Kernforschung
Project Nuclear Safety
75 Karlsruhe
Postfach 3640
Federal Republic of Germany

Professor of Mayinger
Lehrstuhl und Institut fur
Verfahrenstechnik
T.U. Hannover
3000 Hannover 1
Callinstr. 15 F
Federal Republic of Germany

Milad Matthias
Dept. of Nuclear Studies and Safety
Ontario Hydro
700 University Ave. (H-16)
Toronto, Ontario
Canada M5G1X6

Gesellschaft fur Kernforschung (2)
PNS/RBT
75 Karlsruhe
Postfach 3640
Federal Republic of Germany
Attn: Dr. S. Hagen
D. Perinic

H. Seipel
BMFT
Federal Ministry for Research & Technology
53 Bonn
Federal Republic of Germany

Dr. E. Herkommer
Institute for Reactor Safety
5000 Koln 1
Gloschengasse 2
Federal Republic of Germany

Professor Dr. H. Unger
IKE
University of Stuttgart
7 Stuttgart - Vaihingen
Pfaffenwaldring 31
Federal Republic of Germany

W. B. Murfin
PNS
Gesellschaft fur Kernforschung
75 Karlsruhe
Postfach 3640
Federal Republic of Germany

G. H. Kinshin
Safety & Reliability Directorate
Wigshaw Lane
Culcheth
NR Warnington, Cheshire
England

Dr. M. Peehs
KWU
Abt. Rb. 3
852 Erlangen
Postfach 325
Federal Republic of Germany

Dr. M. Dalle Donne (2)
Kernforschungszentrum Karlsruhe
Institut fur Neutronenphysik
und Reaktortechnik
75 Karlsruhe 1
Postfach 3640
Federal Republic of Germany

Dr. H. Kottowski
c/o - Euratom Ispra
21020 Centro Euratom di Ispra
(Varese) Italy

Division of Reactor Safety Research (8)
Office of Nuclear Regulatory Research
U.S. Nuclear Regulatory Commission
Mail Station: G158
Washington, DC 20555
Attn: M. Silberberg, Chief, (10)
Experimental Fast Reactor Safety Branch
R. W. Wright, Experimental Fast
Reactor Safety Branch
R. DiSalvo, Fuel Behavior Branch

U. S. Energy Research & Development Administration (4)
Reactor Safety Research Coordination
Washington, DC 20545
Attn: R. W. Barber, Actg. Director (3)
T. E. McSpadden, Project Manager

Operational Safety Division
U.S. Energy Research & Development Administration
Albuquerque Operations Office
P. O. Box 5400
Albuquerque, NM 87115
Attn: J. R. Roeder, Director

Argonne National Laboratory
9700 South Cass Avenue
Argonne, IL 60439

Oak Ridge National Laboratory
Box Y, Bldg. 9201-3
Oak Ridge, TN 37830
Attn: M. H. Fontana

Brookhaven National Laboratory
Upton, LI, NY 11973
Attn: W. Y. Kato, Head,
Fast Reactor Safety Division

University of California (2)
Energy and Kinetics Department
5530 Boelter Hall
Los Angeles, CA 90024
Attn: W. E. Kastenberg
J. N. Castle

Idaho National Engineering Laboratory
EG&G Idaho, Inc.
P. O. Box 1625
Idaho Falls, ID 83401
Attn: A. W. Cronenberg

University of Arizona (2)
Department of Nuclear Engineering
Tucson, AZ 85721
Attn: R. L. Seale
R. L. Brehm

1200 W. A. Gardner
Attn: K. J. Touryan, 1260
T. B. Lane 1280
1262 H. C. Hardee
1262 D. W. Larson
1262 D. O. Lee
4010 C. Winter

5131 W. B. Benedick
5160 W. Herrmann
5167 B. M. Butcher
5167 J. E. Smaardyk
5167 H. J. Sutherland
5262 K. L. Goin
5400 A. W. Snyder
5410 D. J. McCloskey
5411 D. A. Dahlgren (10)
5411 M. Berman
5411 R. K. Cole
5411 P. W. Conrad
5411 R. L. Knight
5411 J. F. Muir
5412 J. W. Hickman
5412 L. D. Buxton
5420 J. V. Walker
5422 R. L. Coats
5422 H. G. Plein
5423 J. E. Powell
5425 W. J. Camp
5430 R. M. Jefferson
5443 B. D. Zak
5443 L. S. Nelson
5450 J. R. Reuscher
5830 M. J. Davis
5831 N. J. Magnani
5831 T. M. Gerlach
5831 D. A. Powers (20)
5831 R. A. Sallach
5831 F. E. Arellano
5831 A. F. Turbett
5833 F. J. Zanner
5846 E. K. Beauchamp
9330 A. J. Clark, Jr.
9337 N. R. Keltner
8266 E. A. Aas (2)
3141 C. A. Pepmueller (5)
3151 W. L. Garner (3)
For DOE/TIC (Unlimited Release)
3172-3 R. P. Campbell (25)
For DOE/TIC (Unlimited Release)